LEVEL II

REPORT DOCUMENTATION PAGE

READ INSTRUCTIONS
BEFORE COMPLETING FORM

1. REPORT NUMBER	2. GOVT ACCESSION NO.	3. RECIPIENT'S CATALOG NUMBER
Technical Report 80-4	AD-A087 289	TR-81-4

4. TITLE (and Subtitle)	5. TYPE OF REPORT & PERIOD COVERED
Electrical Transport in Doped Polyacetylene,	Interim Technical Report,
	6. PERFORMING ORG. REPORT NUMBER

7. AUTHOR(s)	8. CONTRACT OR GRANT NUMBER(s)
Y.-W. Park, A.J. Heeger, M.A. Druy and A.G. MacDiarmid	N00014-75-C-0962, NSF-DMR76-80914

9. PERFORMING ORGANIZATION NAME AND ADDRESS	10. PROGRAM ELEMENT, PROJECT, TASK AREA & WORK UNIT NUMBERS
Departments of Physics and Chemistry University of Pennsylvania Philadelphia, Pa. 19104	NR-356-602

11. CONTROLLING OFFICE NAME AND ADDRESS	12. REPORT DATE
Department of the Navy Office of Naval Research Arlington, Va. 22217	July 8, 1980
	13. NUMBER OF PAGES
	54

14. MONITORING AGENCY NAME & ADDRESS(if different from Controlling Office)	15. SECURITY CLASS. (of this report)
8 Jul 84	Unclassified
	15a. DECLASSIFICATION/DOWNGRADING SCHEDULE

16. DISTRIBUTION STATEMENT (of this Report)

Distribution unlimited; approved for public release

DTIC
ELECTE
JUL 30 1980
E

17. DISTRIBUTION STATEMENT (of the abstract entered in Block 20, if different from Report)

18. SUPPLEMENTARY NOTES

Prepared for publication in J. Chem. Phys.

19. KEY WORDS (Continue on reverse side if necessary and identify by block number)

transport, polyacetylene, conductivity, thermopower, semiconductor, metal, transition, mobility, solitons, polyene, anisotropic, oriented, hopping, oriented films, dilute limit, transitional region, metallic state, carrier, charge transfer, band theory, delocalized states, disordered polymer, metallic strands, potential barriers

20. ABSTRACT (Continue on reverse side if necessary and identify by block number)

The results of an experimental study of electrical conductivity and thermopower in doped polyacetylene are reported. Included are measurements on both as-grown and partially oriented films doped with iodine and AsF_5; $[CH(AsF_5)_y]_x$ and $[CH(I_3)_y]_x$, where y covers the full doping range. The data indicate three important concentration regimes; the dilute limit (y<0.001), the transitional region (0.001<y<0.01), and the metallic state (y>0.01). In the dilute limit, the transport is via carrier hopping; the mobility is small (~5×10^{-5} cm^2/V sec) and activated ($\Delta E = 0.3$ eV). The semiconductor to metal transition is evident in the data (over)

DD FORM 1473 EDITION OF 1 NOV 65 IS OBSOLETE
1 JAN 73
S/N 0102-014-6601 |

278950

80 7 21 024

20. and leads to a qualitative change in temperature dependence of the conductivity and to finite zero temparture values above $y_c \simeq 0.01-0.02$. The transport mobility increases by five to six orders of magnitude on going through the transitional region. In the metallic state, the high mobility (~ 60 cm^2/V sec, assuming unit charge transfer) provides evidence of the validity of a band theory approach with delocalized states in this disordered polymer. The transport in the metallic state is described as metallic strands separated by thin potential barriers. The main effect of orientation appears to be to alter the barriers. In particular, use of oriented cis-(CH)$_x$ starting material leads to significant improvement in conductivity due to smaller barrier widths and lower barrier heights. Analysis of the temperature dependence of the conductivity within this model leads to an estimate of the intrinsic conductivity in heavily doped metallic $[CH(AsF_5)_4]_x$, $\sigma \simeq 4 \times 10^4$ ohm^{-1}cm^{-1} at room temperature.

Electrical Transport in Doped Polyacetylene

by

Y.W. Park, A.J. Heeger, M.A. Druy[*]
and A.G. MacDiarmid[*]

To be published

in

J. Chem. Phys.

Accession For		
NTIS GRA&I	☑	
DDC TAB	☐	
Unannounced	☐	
Justification		
By		
Distribution/		
Availability Codes		
Dist	Avail and/or special	
A		

Departments of Physics and Chemistry[*]
University of Pennsylvania
Philadelphia, Pa. 19104

July 8, 1980

ELECTRICAL TRANSPORT IN DOPED POLYACETYLENE[*]

Y.-W. Park and A. J. Heeger
Department of Physics
and
Laboratory for Research on the Structure of Matter

and

M. A. Druy and A. G. MacDiarmid
Department of Chemistry
and
Laboratory for Research on the Structure of Matter
University of Pennsylvania
Philadelphia, Pennsylvania 19104

Abstract

The results of an experimental study of electrical conductivity and thermopower in doped polyacetylene are reported. Included are measurements on both as-grown and partially oriented films doped with iodine and AsF_5; $\left(CH(AsF_5)_y\right)_x$ and $\left(CH(I_3)_y\right)_x$ where y covers the full doping range. The data indicate three important concentration regimes; the dilute limit (y < 0.001), the transitional region (0.001 < y < 0.01), and the metallic state (y > 0.01). In the dilute limit, the transport is via carrier hopping; the mobility is small ($\sim 5 \times 10^{-6}$ cm^2/V-sec) and activated ($\Delta \epsilon = 0.3$ eV). This localized state hopping is consistent with the proposed soliton doping mechanism. The semiconductor to metal transition is evident in the data and leads to a qualitative change in

temperature dependence of the conductivity and to finite zero temperature values above $y_c \simeq 0.01 - 0.02$. The transport mobility increases by five to six orders of magnitude on going through the transitional region. In the metallic state, the high mobility (~ 60 cm^2/V-sec, assuming unit charge transfer) provides evidence of the validity of a band theory approach with delocalized states in this disordered polymer. The transport in the metallic state is described as metallic strands separated by thin potential barriers. The main effect of orientation appears to be to alter the barriers. In particular, use of oriented cis-(CH)$_x$ starting material leads to significant improvement in conductivity due to smaller barrier widths and lower barrier heights. Analysis of the temperature dependence of the conductivity within this model leads to an estimate of the intrinsic conductivity in heavily doped metallic $[CH(AsF_5)_y]_x$, $\sigma \simeq 4 \times 10^4$ Ω^{-1}-cm^{-1} at room temperature.

I. INTRODUCTION

Linear polyacetylene, $(CH)_x$, is the simplest conjugated organic polymer and is therefore of special fundamental importance. Interest in this semiconducting polymer has been stimulated by the successful demonstration of doping with associated control of electrical properties over a wide range; the electrical conductivity of films of $(CH)_x$ can be varied over 12 orders of magnitude from that of an insulator $(\sigma \sim 10^{-9}\,\Omega^{-1}\,cm^{-1})$ through semiconductor to a metal $(\sigma \sim 10^3\,\Omega^{-1}\,cm^{-1})$.[1,2] Various electron donating or accepting molecules can be used to yield n-type or p-type material, and compensation and junction formation have been demonstrated.[3,4] Optical-absorption studies[5,6] indicate a semiconductor with peak absorption coefficient of about 3×10^5 cm^{-1} at 1.9 eV. Partial orientation of the polymer fibrils by stretch elongation of the $(CH)_x$ films results in anisotropic electrical[7] and optical properties[6] suggestive of a highly anisotropic band structure.[8] The electrical conductivity of partially oriented metallic $[CH(AsF_6)_{0.1}]_x$ is in excess of 2000 $\Omega^{-1}\,cm^{-1}$.

The qualitative change in electrical and optical properties at dopant concentrations above a few percent have been interpreted[2] as a semiconductor-metal transition by analogy to that observed in studies of heavily doped silicon. However, the anomalously small Curie-law susceptibility components in the lightly doped semiconductor regime[9] suggest that the localized states induced by doping below the semiconductor-metal transition are nonmagnetic. These observations coupled with electron

spin resonance studies of neutral defects in the undoped polymer have[10,11]
resulted in the concept of soliton doping; i.e. localized domain-wall-like[12,13]
charged donor-acceptor states induced through charge transfer doping.

The initial results obtained on conducting polymers have generated interest from the point of view of potentially low cost solar energy conversion. Experiments utilizing polyacetylene, $(CH)_x$, successfully demonstrated rectifying junction formation.[3,4,14] In particular a p-$(CH)_x$:n-ZnS heterojunction solar cell has been fabricated with open circuit photovoltage of 0.8 Volts.[4] In related experiments, a photoelectrochemical photovoltaic cell was fabricated using $(CH)_x$ as the active photoelectrode.[15]

In this paper we present the results of a detailed experimental study of the electrical transport, conductivity (σ) and thermoelectric power (S), in $(CH)_x$ doped with AsF_5 and iodine. The experimental results cover the full concentration (y) range from undoped to metallic on both partially oriented and as-grown films. The experimental techniques, including sample preparation, doping and measurement of $\sigma(T,y)$ and $S(T,y)$, are described in Section II. The results are presented in Section III and analyzed in Section IV in terms of transport in the three concentration regimes: metallic, semiconductor-metal (SM) transition, and lightly doped semiconductor. A summary and conclusion are given in Section V.

II. EXPERIMENTAL TECHNIQUES

a) Samples

Crystalline films of polyacetylene were grown in the presence of a Ziegler catalyst using techniques similar to those developed by Shirakawa et al.[16-20] X-ray diffraction and scanning electron micrograph studies show that the as-grown films, both cis and trans, are polycrystalline and consist of matted fibrils which are typically 200 Å in diameter.[16-20] Recent electron microscopy studies[22] of thin $(CH)_x$ films polymerized directly on an electron-microscope grid have shown that the fibrillar structure is the nascent morphology. The measured density of the as-grown film is ca. 0.4 gm/cm³[16-20,21] compared with 1.2 gm/cm³ as obtained by flotation techniques, indicating that the volume filling fraction, f, of fibrils is approximately 1/3.

The cis-trans content was controlled by thermal isomerization.[15-19] Samples used in these studies were films (typical thickness ~ 0.1 mm) taken from the side wall of the reactor. All measurements were carried out on either ~90% cis (synthesized at -78° C) or 95% ~ 98% trans (after thermal isomerization for 2 hrs at 200° C). The cis-trans content was monitored by examination of infrared spectra.[16-20] Care was taken to achieve pure $(CH)_x$ starting material through extensive washing to remove all catalyst, with subsequent storage and handling either in vacuum or in inert atmosphere to minimize oxygen content. Chemical analysis of typical cis and trans $(CH)_x$ indicate analytical purity.[*]

---

[*] Films used had elemental analyses in the range:
   C = 90.91%, H = 7.91% (total 98.82%) to
   C = 91.80%, H = 7.99% (total 99.79%);
calculated values for $(CH)_x$: C 92.26%; H 7.74%.

Partially aligned films were obtained by mechanical stretching.[21,23]

It was found that when cis-films of polyacetylene were extended in an inert

(argon) atmosphere, ultimate extension ratios as high as 3.3 were obtained;

subsequent thermal isomerization under stress resulted in $l/l_o \sim 4$ where

l_o and l are the initial and final lengths of the film. Oriented films used

in this study had $l/l_o \sim 3$. Details on the stretch orientation and the tensile

properties of $(CH)_x$ are reported elsewhere.[21]

b) Doping

Doping was carried out by exposing the $(CH)_x$ films to vapor of

iodine or AsF_6.[1-4,24] In the case of the iodine doping, the vapor was carried by

a flow of dry N_2 gas; the dry nitrogen was first passed through a vessel

containing iodine crystals at room temperature and then the gas was flowed

over the $(CH)_x$ films to be doped. Doping rates could be varied by con-

trolling the temperature (and vapor pressure) of the iodine as well as

controlling the flow rate (typically 0.1 cubic feet per hour). Slow, controlled

doping with AsF_6 was achieved by cooling the AsF_6 with a slush bath to

ca. $-100^\circ C$ to reduce its vapor pressure. The AsF_6 doping was carried

out in stages. In the initial stage, the sample was exposed to ≤ 0.5 torr

of AsF_6. This pressure was subsequently increased in stages. The final

pressure used was dependent on the desired dopant concentration; for

heavily doped metallic $[CH(AsF_6)_y]_x$, $y \sim 0.1$, the final pressure was

approximately 5 torr.

Specific concentrations were achieved by monitoring the conductivity of the sample (or a reference sample in the container) and comparing it with the previously calibrated curve of conductivity (room temperature) vs. concentration. The doping process was stopped when the conductivity reached the desired value. The dopant concentration was determined by weight uptake; concentrations have previously been verified by chemical analysis.[1] Samples were pumped for about 1-2 hrs under dynamic vacuum after doping, with no observable change in conductivity.

The uniformity of the doping on the microscopic scale has been studied by a variety of techniques. In the case of iodine, X-ray studies,[25] variation of the proton nuclear magnetic resonance (nmr) second moment,[26] and photoemission results[27] are consistent and imply essentially uniform doping throughout the polymer fibrils. For AsF_5, photoemission results[28] imply non-uniformity at high concentrations with a higher concentration near the surface of the fibrils. At AsF_5 concentrations below 1%, the photoemission data[28] indicate penetration of the dopant into the bulk of the fibrils.

In general, doping the cis isomer appears to give consistently higher conductivity values (about two to five times greater) than the trans isomer even though the trans isomer has a higher room temperature conductivity ($\sim 2 \times 10^{-5} \Omega^{-1} cm^{-1}$) than the cis-isomer ($\sim 2 \times 10^{-9} \Omega^{-1}-cm^{-1}$). Optical absorption,[29] thermopower,[30] and nmr 2nd moment studies[26] indicate

that cis-trans isomerization takes place during iodine doping. Thus, the same final product is obtained from both isomers when they are heavily doped, and that product is primarily trans-(CH)$_x$. It is not yet clear to what extent AsF$_5$ doping induces similar isomerization. The higher conductivities obtained with cis starting material suggest that the doping induced isomerization leads to higher quality trans material than thermal isomerization with subsequent doping.

c) Electrical Conductivity Measurements

All conductivity measurements utilized four-probe techniques. The values given were obtained directly from the measured resistance and the measured sample dimensions. No corrections have been made for the low density associated with the fibrillar structure of the (CH)$_x$ films.

Due to the chemical activity of iodine and AsF$_5$, the sample holders were made with glass frames and utilized platinum leads; Electrodag was used to make the electrical contacts onto the polymer samples. Typically, the contacts were applied in air with exposure time kept to a minimum; the mounted samples were pumped in vacuum for 2-3 hours until the contacts were dry. The effect of the solvent in the Electrodag paint was checked by applying the contacts before and after doping. The metallic conductivity of samples mounted before doping was typically 50% higher than that of the samples whose contacts were applied after the samples were doped. In addition to Electrodag, gold evaporated contacts and mechanical (pressed) contacts have been tried. The various contacts yield conductivity data

which are consistent and without significant differences. The effects of different contacts have also been studied by Kwak et al.[31] The conductivity data presented in this paper were obtained from samples mounted before doping, unless otherwise stated. Contacts were checked to be ohmic for currents from 10^{-10} - 10^{-5} amps for undoped $(CH)_x$, and from 10^{-6} - 10^{-2} amps for metallic samples.

To check the effect of the air exposure on the undoped $(CH)_x$, an on-line experiment was set up to monitor conductivity vs. time. Samples were mounted in a glove bag under argon atmosphere. In the first three hours of air exposure, the conductivity of cis-$(CH)_x$ increased by one order of magnitude while that of trans-$(CH)_x$ increased by only about a factor of three. Upon pumping out the air, the conductivity returned to its initial value. Such reversibility was also observed earlier in electron spin resonance experiments.[10] Air exposure of heavily doped metallic samples for 2 hours resulted in a 40% and 20% decrease, respectively, for $[CH(AsF_5)_y]_x$ and $[CH(I_3)_y]_x$. Studies of the effect of oxygen on metallic $[CH(I_3)_y]_x$ samples showed a decrease in conductivity of about 10% in the first four hours.

In an initial attempt to stabilize the samples after doping, paraffin wax coatings were applied. Conductivity measurements of uncoated and wax coated metallic $[CH(I_3)_y]_x$ were carried out on samples doped at the same time and under identical conditions. The conductivity of the wax coated sample decreased only 10% after 12 hours, whereas the conductivity of the uncoated sample fell by a factor of five during the same period.

Similar tests were carried out in connection with the temperature dependence measurements. The temperature dependence exhibited by doped samples obtained from the bottom of the reactor was not significantly different from that obtained from samples extracted from the side walls. Using cis samples of either origin, metallic AsF_5-doped $(CH)_x$ showed a slight increase in conductivity (a few per cent) below room temperature as noted previously.[32] Samples mounted after doping, or samples re-painted with solvent containing Electrodag, showed a monotonic decrease in conductivity with decreasing temperature. Exposure to air had similar effects; the weak maximum reduced in magnitude and shifted toward higher temperature before disappearing after ~ 30 minutes exposure. The wax coated samples showed similar temperature dependences to those of the uncoated ones.

d) Thermopower Measurements

A rectangular sample (3mm x 25mm) was cut from the polymer film and mounted lengthwise between two copper blocks using pressure contacts. The temperature difference (ΔT) was established by heating one of the copper blocks and the voltage (generated by the thermal gradient across the sample) was measured. Typically $\Delta T \sim 2K$ was used during each measurement, so that the thermopower is an average over this interval. The measurement of ΔT across the sample utilized a copper-constantan differential thermocouple. The thermodynamically stable

trans-(CH)$_x$ was used in all the thermopower measurements. The iodine

and AsF$_5$ concentrations in the doped samples were determined as described

above. Reproducibility for independently prepared samples was about ±10%

at the lightest doping levels and better than ±5% in the metallic regime.

Due to the extremely rapid increase of the conductivity at low dopant levels,

the uncertainty in y was ±0.001 for concentrations below y = 0.01 (1 mole %).

Even at the highest dopant levels, the accuracy in y was always better than

±0.005.

III. EXPERIMENTAL RESULTS

a) Thermopower

The room temperature results, S vs log y for trans-[CH(I$_3$)$_y$]$_x$

are shown in Fig. 1. The sign of S is positive throughout the entire con-

centration range indicating p-type behavior consistent with charge transfer

doping to the iodine acceptor and the formation of I$_3^-$. The semiconductor-

metal transition is clearly evident in Fig. 1. Note that S is relatively

insensitive to the dopant concentration up to approximately y = 0.001. For

the undoped trans-(CH)$_x$, S = (900 ± 50) μV/K and then decreases slightly

to S = (750 ± 50) μV/K at y = 0.001. Figure 1 shows the earlier

data[30] in more detail with additional points in the transitional region.

As shown in our previous paper,[30] within the measurement accuracy, the

thermopower is independent of temperature in the lightly doped regime

(y ≤ 0.001). At concentrations above the SM transition, S decreases with

decreasing temperature.[30]

The thermopower in the metallic limit is shown in Fig. 2, including the results for both unoriented cis-$[CH(AsF_5)_{.147}]_x$ and partially oriented trans-$[CH(AsF_5)_{.096}]_x$ with $l/l_o = 3.2$. Any variation between oriented and unoriented samples is comparable to the variations observed from sample to sample (indicated by error bars on Fig. 2). No qualitative difference and no significant anisotropy are observed; S(T) is essentially the same for oriented and as-grown samples. This is consistent with expectations. Since thermoelectric power is a zero-current transport coefficient, interfibril contacts should be unimportant allowing an evaluation of the intrinsic metallic properties. The magnitude and temperature dependence of S (Fig. 2) are characteristic of a degenerate electron gas and are indicative of intrinsic metallic behavior.[30,31]

For dilute concentrations well below the semiconductor-metal transition the thermopower is large and essentially temperature independent. Such behavior can be understood for a dilute concentration of carriers (holes) which hop among a set of localized states. In this case, where the kinetic energy of the carriers is negligible, the thermopower is given by the Heikes formula[33,34]

$$S = +\frac{k_B}{|e|} \ln[(1-\rho/\rho]$$ (1)

where $\rho = n/N$ is the ratio of the number of holes (n) to the number of available sites (N) (eq. 1 assumes spinless carriers; the inclusion of spin degeneracy[34] changes the expression to $S = +(k_B/|e|)\ln(2-\rho)/\rho$). Identification

with the experimental data for undoped <u>trans</u>-$(CH)_x$ requires that $\rho \simeq 10^{-4}$

and temperature independent. This value corresponds to a carrier concen-

tration of $2 \times 10^{18} cm^{-3}$ in "undoped" $(CH)_x$ and is consistent with the results

of capacitance vs voltage studies[35] of p-$(CH)_x$:n-CdS heterojunctions using CdS

with known carrier concentration. The results therefore imply that in the

undoped polymer, the conductivity is due to a small number of residual carriers

$(\rho_0 \simeq 10^{-4})$ provided by defects and/or impurities, and that the mobility results

from hopping. The insensitivity of the thermopower to iodine concentrations

less than 0.1 mole% (or 0.1% I_3^-) is consistent with this interpretation and

implies that ρ_0 is well below 10^{-3}. From eq. 1, the thermopower at

$y = 10^{-3}$ should be 0.75 of that at $y = 10^{-4}$; consistent with Fig. 1 to within

the combined uncertainty in y and ρ.

b) Conductivity

By careful control of the dopant concentration, any specified conduc-

tivity can be obtained covering the range from $\sigma = 2 \times 10^{-9} \, \Omega^{-1}$-$cm^{-1}$ to

$\sigma > 10^3 \, \Omega^{-1}$-$cm^{-1}$ using <u>cis</u>-$(CH)_x$ starting material. Higher metallic values,

$\sigma > 3000 \, \Omega^{-1}$-$cm^{-1}$, were obtained using <u>cis</u> starting material, stretch-

oriented ($\ell/\ell_0 = 3.1$) and then doped with AsF_6. Since exposure of undoped

$(CH)_x$ to ammonia vapor[2] decreases σ to values below $10^{-10} \, \Omega^{-1}$-cm^{-1}, the

accessible range covers more than thirteen orders of magnitude.

The temperature dependences of AsF_6-doped $(CH)_x$, both as-grown,

and stretch-oriented are shown in Fig. 3, for a variety of dopant concen-

trations. The temperature range covered by the measurements depended

on the resistance of the sample; for the highest conductivity sample, data

were obtained over the entire range from 300 to 1.8 K. The curvature

seen in log σ vs $1/T$ was noted earlier for halogen dopants.[35] This curvature

may arise from disorder, for example, leading to a distribution of activation

energies.[36] Alternatively variable range hopping may play a role at low

temperatures. Taking the initial slope of the log σ vs $1/T$ plots, we obtain

the activation energy, ΔE, which serves as a simple index of the conduc-

tivity behavior. The results are presented in Fig. 4 where data from

AsF_5-doped samples and iodine doped samples are plotted versus concen-

tration on a logarithmic scale. Note that the iodine doped samples are

formulated as $[CH(I_3)_y]_x$ since the I_3^- ion is known to be present.[37] Using

this formulation the data from the two dopants are in good agreement,

although the AsF_5 doped samples give consistently lower activation energies

above $y = 0.01$ consistent with the higher metallic conductivity. The

activation energy of the undoped trans-$(CH)_x$ is $\Delta E = (.3 \pm .03)$ eV. ΔE is

relatively insensitive to the dopant concentration up to $y = 0.001$, and then

decreases rapidly through the SM transition. Above $y = 0.01$ (1 mole %)

ΔE is small and nearly independent of the concentration; the conductivity

is no longer activated in heavily doped $(CH)_x$.

The room temperature values from Fig. 3 are replotted as σ vs y in

Fig. 5. The value $y = 10^{-4}$ for undoped $(CH)_x$ was determined from the

magnitude of the thermopower, as described above;[34] the point at $y = 0.003$

was determined by weight uptake. In the dilute concentration regime, σ

increases approximately in proportion to the dopant concentration, so that

the mobility is independent of y. Note that in this dilute regime, the

activation energy (Fig. 4) is also insensitive to the dopant concentration.

Figures 4 and 5, together with the temperature independence of the thermo-

power, [30] imply that in the dilute regime the transport is via carrier hopping;

the conductivity results from a temperature independent carrier concentration

(proportional to y) and an activated mobility. [38]

The temperature dependence of the conductivity in the metallic

high concentration limit is shown more clearly in Figure 6, where σ/σ_{RT}

vs. T is plotted in a linear scale. The room temperature conductivity

values for these partially oriented films were measured independently by

simple four-probe and by Montgomery[39] techniques. The results, com-

pared in Table 1, are in general agreement. For heavily doped metallic

$[CH(AsF_5)_{0.14}]_x$ (oriented with $l/l_0 = 3.1$), the conductivity first increases

on cooling below room temperature,[7,31] goes through at maximum at 220 K,

then decreases and becomes constant below 5 K with $\sigma(0)/\sigma(300 K) = 0.66$.

The conductivity maximum near room temperature varies from sample to

sample, but in general cis-$(CH)_x$ starting material leads to a larger

maximum than trans-$(CH)_x$. Also shown in Fig. 6 are the results for

$[CH(I_3)_{.08}]_x$ ($l/l_0 = 3.1$). The conductivity decreases monotonically and

appears to be going to zero as $T \to 0$. The low temperature data from

these samples are shown in more detail in Fig. 7 where we plot the

normalized conductivity (log scale) vs $1/T$. For the metallic $[CH(AsF_5)_{0.14}]_x$,

the conductivity at low temperatures[31] approaches the constant value,

$\sigma(0) \simeq 800 \ \Omega^{-1}$-$cm^{-1}$. For the iodine doped $[CH(I_3)_{0.08}]_x$, the low temperature conductivity continues to be activated, even though the room temperature value is comparable to that of the AsF_5 doped sample.

Considering the matted fibril structure of polyacetylene the temperature independence of the conductivity (see Fig. 7) suggests a tunneling mechanism through the interfibril contact barriers in addition to the thermally activated charge transfer over the barriers located between large metallic conducting fibers. The residual activation for heavily doped $[CH(I_3)_y]_x$ is not understood. However, this may indicate that even the heavily iodine doped samples are only just on the verge of metallic behavior.

The temperature dependence of the conductivity of trans-$[CH(AsF_5)_{0.10}]_x$ samples, both partially oriented with elongation ratio $l/l_o = 2.8$ and unoriented, are shown in Fig. 8. The two samples were prepared from the same starting material and were doped simultaneously. The temperature dependences of the normalized conductivities are similar although the room temperature values varied considerably (for $l/l_o = 2.8$, $\sigma_\parallel = 1400 \ \Omega^{-1}$-$cm^{-1}$ and $\sigma_\perp = 280 \ \Omega^{-1}$-$cm^{-1}$; for $l/l_o = 1$, $\sigma_\parallel = \sigma_\perp = 240 \ \Omega^{-1}$-$cm^{-1}$). Furthermore, at low temperatures all four samples approach nearly temperature independent behavior as shown in Fig. 9. The low temperature normalized values are somewhat higher in the oriented samples. These results indicate that the role of the interfibril contact barriers are similar in each direction, and that the barrier height and/or widths are slightly

smaller for the partially oriented films. The temperature dependence of

σ for a partially oriented film ($\ell/\ell_o \sim 3$) which has been exposed to the air

during the isomerization under stress, flattens more slowly resulting in

$\sigma(1.8 \text{ K})/\sigma(300 \text{ K}) = 10^{-2}$. Combined with the observation of decreasing

tensile strength after air exposure, this result suggests that the cross

linking induced by the air exposure makes the interfibril contact barriers

effectively larger.

Although the temperature dependences of the normalized conduc-

tivities are the same, the room temperature conductivity in the parallel

and transverse direction of the partially aligned films are different about

factor of five for the $\ell/\ell_o = 2.8$ sample of Figs. 8 and 9. Since the

interfibril contact barriers are same in either direction, the large

difference in absolute magnitude is evidently due primarily to the difference

in total number of chains in the respective directions. Since the films are

not perfectly oriented, there are chains going along the transverse direction

in the partially oriented films. Thus, more complete orientation can be

expected to yield larger values for $\sigma_{\parallel}$ and for the anisotropy $\sigma_{\parallel}/\sigma_{\perp}$. In

this context, the thermopower data of Fig. 2 are readily understood. Even

in the transverse direction $\sigma_{\parallel}$ dominates the transport so that S is deter-

mined by $S_{\parallel}$.[40] Determination of $S_{\perp}$ will require nearly complete orientation.

The temperature dependences of the normalized conductivity of

trans-$[CH(AsF_5)_y]_x$ films are shown in Fig. 10 with values of y spanning

the SM transition. The films were partially oriented to minimize interfibril

contact effects. A qualitative change in behavior is observed at the SM

transition ($y = y_c$). At low concentrations the curves appear thermally

activated and $\sigma \to 0$ as $T \to 0$. Above y_c, the curvature changes and the

conductivity remains finite as $T \to 0$. The low temperature normalized

conductivity appears to be an excellent indicator of the SM transition in

AsF_5 doped $(CH)_x$ as shown in Fig. 11. From Fig. 11 we infer $y_c \simeq 0.01 - 0.02$.

Note that, as described above, for the iodine doped samples it appears

that $\sigma \to 0$ as $T \to 0$ even at the highest doping levels. Thus, either the

interfibril barrier effects are significantly more important or the metallic

state is not truly achieved even at the highest doping levels.

IV. DISCUSSION

a) Semiconductor-Metal Transition; Mobility

The transition from semiconductor to metal is most clearly evident

in the normalized conductivity data of Figs. 10 and 11 obtained from partially

oriented films. The qualitative change in temperature dependence and

finite zero temperature values above $y_c \simeq 0.01 - 0.02$ are indicative of an

abrupt change in behavior as a function of dopant concentration. For

iodine doping the situation is somewhat less clear as noted by others[41] and

described in Section IIIb.

We note that the critical concentration, y_c, for the SM transition,

as inferred from the conductivity data of Figs. 10 and 11, appears to be

somewhat below that inferred from the onset of Pauli susceptibility;[9] from

the conductivity data we infer $0.01 < y_c < 0.02$, whereas the susceptibility

data suggest $y_c > 0.02$. Additional susceptibility studies are underway to

provide a more detailed and accurate description of the transitional regime.

Direct measurements of the mobility (e.g. time of flight, etc.)
are not available. Although Hall effect data have been reported in the[42]

metallic regime, the Hall coefficient is two orders of magnitude below

that expected on the basis of approximately one carrier per dopant and

may be dominated by the fibril structure of the composite medium. Some

important information on the transport mobility in the semiconductor and

metallic limits can be obtained directly from the conductivity.

In lightly doped trans-$(CH)_x$, the mobility is activated as described

in Section IIIb with a room temperature value of $\mu \equiv \sigma/ne \sim 5 \times 10^{-5} \, cm^2/V$-secs

(see Fig. 12). For $y > 0.003$, one finds a dramatic increase in μ. At

higher dopant levels (i.e. in the transitional regime) ΔE is changing so

that it is not possible to extract μ from the conductivity.

In the metallic regime, e.g. $[CH(AsF_5)_{0.1}]_x$ the number of carriers

can be estimated by assuming unit charge transfer per dopant or from the

oscillator strength as obtained from optical studies.[29] The latter results

suggest that in the heavily doped metallic state all the π-electrons contribute

to the metallic transport; thus $n(metal) \sim 2 \times 10^{22} \, cm^{-1}$. Taking the intrinsic

conductivity to be $\sigma^{dc}_{intrinsic} \gtrsim 2 \times 10^6 \, \Omega^{-1}$-$cm^{-1}$ as inferred from analysis

of the optical data,[29] one obtains $\mu(\text{metal}) \geq 6 \text{ cm}^2/\text{V-sec}$. Note that

assuming that all π-electrons contribute requires that heavy doping removes

the bond-alternation leading to a uniform bond length polyene. Taking the

somewhat more conservative point of view of one carrier per dopant, the

corresponding value for $[CH(AsF_5)_{0.1}]_x$ would be $n \sim 2 \times 10^{21}$ with $\mu \geq$

$60 \text{ cm}^2/\text{V-sec}$. This latter value is plotted in Fig. 12 as characteristic of

the metallic state.

Although there is considerable uncertainty in the absolute values

in both limits, the results nevertheless demonstrate a remarkable change

in mobility, five or six orders of magnitude, on going through the trans-

itional region. This large increase in μ *represents perhaps the clearest*

indication of a major change in electronic structure and/or transport

mechanism at the SM transition in doped polyacetylene.

b) Metallic State

The high mobility in the metallic state is unexpected in view of the

extensive disorder; the doped polymer is only partially crystalline and

contains $\sim 10\%$ charged impurities in random interchain positions. Given

the considerable evidence of one-dimensionality from transport,[7] optical[6,29]

and nmr studies,[43] the effects of disorder would be expected to be particularly[44]

large.

The thermopower data in the high concentration limit provide

independent information on the metallic state and are consistent with

metallic behavior.[30,31] For a nearly filled band (i. e. p-type) metallic system,

the thermopower can be written as

$$S = +\frac{\pi^2}{3} \left(\frac{k_B}{|e|}\right) kT \left[\frac{d\ln\sigma(E)}{dE}\right]_{E_F} \qquad (2)$$

where $\sigma(E) = n(E)|e|\mu(E)$ and $n(E)$ is the number of carriers contributing

to $\sigma(E)$, $dn(E)/dE = g(E)$ is the density of states (both signs of spin) and

$\mu(E)$ is the energy dependent mobility. Assuming energy independent

scattering ($\mu(E)$ independent of E)

$$S = +\left(\frac{k_B}{|e|}\right) \frac{\pi^2}{3} k_B T \eta(E_F) \qquad (3)$$

where $\eta(E_F) = g(E_F)/N$ is the density of states per carrier. As indicated

in Fig. 2 and in earlier papers,[30,31] S is a linear function of T for AsF_5-doped

metallic $(CH)_x$ whereas for heavy iodine doping there is curvature in S vs T.

Nevertheless, in both cases, the thermopower decreases smoothly toward

zero as $T \to 0$ in a manner typical of metallic behavior even at temperatures

as low as 2 K. The experimental results (Fig. 2) are in good agreement

with eq. 3 with $\eta(E_F) = 1.36$ states per eV per carrier. Since there are

0.15 carriers per carbon atom in $[CH(AsF_5)_{0.15}]_x$ (assuming complete

charge transfer), the thermopower data yield for the density of states,

$g(E_F) \sim 0.2$ states per eV per C atom in good agreement with the value

obtained from magnetic susceptibility measurements.[9]

Although the conductivity is weakly activated below 50 K and becomes temperature independent at low temperatures, the thermopower data imply intrinsic metallic behavior at all temperatures. We therefore conclude that the dc transport is limited by interfibril contacts, and that the heavily doped polymer can be described as consisting of metallic strands separated by thin potential barriers. This is consistent with optical studies[29] which indicate that the intrinsic individual strand conductivity is much higher than the dc value.

A model appropriate to a composite medium consisting of metallic particles dispersed at high density in an insulating matrix was recently developed by Sheng et al.[45] Fluctuation induced tunneling through potential barriers leads to the bulk dc conductivity at low temperatures with activation over the barriers at higher temperatures. We identify the conducting aggregates of Sheng et al.[45] with the metallic fibrils and assume that the barriers are due to interfibril contacts. Sheng et al.[45] assume a parabolic barrier, $V = V_o - (4V_o/W)x^2$, where V_o and W are the barrier height and thickness, respectively. We assume the cross sectional area, A, of the barriers is typically equal to that of the polymer fibrils whose diameter is ~ 200 Å. In terms of these parameters, the conductivity (σ_j) of the junction can be expressed as

$$\sigma_j(T) = \sigma_o e^{-\frac{T_1}{T + T_o}} \tag{4}$$

where

$$T_1 = \frac{2 A V_o^2}{\pi e^2 k_B W} \tag{5}$$

and

$$T_o = \frac{4\hbar A V_o^{3/2}}{\pi^2 e^2 k_B (2m)^{\frac{1}{2}} W^2} \tag{6}$$

The parameters T_1 and T_o are obtained experimentally from the slope and intercept, respectively, of plots of $[\ln(\sigma/\sigma_{RT})]^{-1}$ vs T as shown in Fig. 13. The results are summarized in Table 2. Typical values for T_1 and T_o are comparable and lead to barrier thickness of 10 - 20 Å and barrier heights of order $3 - 7 \times 10^{-3}$ eV. The main effect of orientation appears to be the alteration of the barrier parameters. For example, doping with oriented cis-(CH)$_x$ starting material significantly reduces both the barrier thickness and the barrier height. With this model, the dc conductivity in the metallic state can be viewed as resulting from resistors in series. The metallic strands are in series with the junctions, so that $R_{dc} = R_i(T) + R_j(T)$ where $R_i(T)$ results from the doped metallic strands with an intrinsic metallic conductivity, and R_j is the junction resistance. Assuming $R_i(T) = aT$ (near room temperature) and $R_j = R_o \exp[T_1/T + T_o]$, the magnitude of the conductivity maximum in the data of Figs. 6 and 10 implies that $R_i/R_j < 10^{-1}$ at room temperature. We thereby obtain an estimate of the intrinsic conductivity in heavily doped metallic $[CH(AsF_5)_y]_x$, $\sigma(300 \text{ K}) \simeq 4 \times 10^4 \ \Omega^{-1}\text{-cm}^{-1}$.

c) Light Doping, y < 0.001

In this low concentration regime, the number of carriers is proportional to the concentration of dopants, and the activation energy remains constant. Moreover, the temperature independent thermopower indicates a temperature independent carrier concentration implying that the mobility is activated. We therefore conclude that in the dilute regime

$$\sigma = ne\mu \tag{7}$$

where n is the number of carriers (equal to the number of dopants) and the mobility is given by

$$\mu = \mu_o e^{-\Delta E/kT} \tag{8}$$

with $\Delta E = 0.3$ eV as indicated on Fig. 4. Such a small, thermally activated mobility is unexpected in a broad bandwidth semiconductor like $(CH)_x$. Although one might suggest that the activated transport is limited by disorder in the polymer, the high conductivity and high mobility in the metallic state argue to the contrary. One might argue that the observed activation energy is the result of int fibril contact resistance. However, the activation energy is inse tive to whether the polymer is taken as-grown or stretch-oriented. (Note that the low temperature results in the metallic regime show major changes in interfibrillar contact effects on orientation; see Figs. 7, 8, and 9). Moreover, nearly identical results are obtained

from low density foam-like material synthesized using a gel as an intermediate step; whereas the fibril density is down by more than an order of magnitude, and the fibril diameter is three to five times larger.[46]

The localized state hopping transport inferred from the thermopower measurements below y = 0.001 is qualitatively consistent with the proposed[9,30,47] soliton doping mechanism. Motion of the charged localized domain-walls would be expected to be via diffusive hopping in agreement with the low mobility inferred from Fig. 5 for y < 0.001. Moreover, for a fixed impurity concentration the number of charged kinks would be independent of temperature in agreement with the temperature independent thermopower found in the dilute limit. Finally, although the domain-wall would be distributed over a group of carbon atoms, the center of mass of the wall could take any position along the chain so that the number of available sites would be of order the number of carbon atoms in agreement with the magnitude of the thermopower.

The formation of domain-walls, or solitons on long chain polyenes has been studied theoretically by Rice[12] and by Su, Schrieffer and Heeger.[13] The electronic structure of the soliton exhibits a localized state φ_0 at the center of the gap, containing one electron for the neutral kink. While this localized state is spin unpaired, the distorted valence band continues to have spin zero. Thus, the neutral soliton has spin 1/2. The static susceptibility therefore will contain a Curie law contribution and can be used to count the number of neutral soliton defects present. Spin

resonance linewidth[11] and nmr relaxation[43] studies have demonstrated mobile

spin species spread out over many lattice constants in agreement with

these ideas. The number of unpaired spins, typically one per 3000 carbon

atoms is comparable to the number of charge carriers in the undoped

polymer ($\sim$ one per 10,000 carbon atoms) inferred from the thermopower.

Since the localized state occurs at the gap center, i.e. the chemical

potential, the relevance of the solitons to the doping of $(CH)_x$ depends on

the energy for creation of a soliton, E_s, as compared with the energy

required for making an electron or a hole, $\frac{1}{2}Eg = \Delta$. Numerical estimates[13]

indicate that soliton formation is energetically favorable, i.e. $E_s < \Delta$.

Moreover, Takayama et al.[48] have recently developed a continuum model

in which they find $E_s = \frac{2}{\pi}\Delta$; i.e. always less than Δ.

From these observations we suggest that in the undoped trans-$(CH)_x$,

a fraction of the isomerization induced defects has been ionized by residual

impurities to give the observed density ($\rho \sim 10^{-4}$). Subsequent doping will

ionize more and/or create additional charged kinks.

In the case of diffusive hopping, the mobility is given by the

Einstein relation, $\mu = eD/kT$, where D is the diffusion constant. To obtain

an estimate of the diffusion constant we use the result of Wada and

Schrieffer[49] (WS) for one-dimensional Brownian motion of domain-walls in

contact with thermal phonons

$$D_{WS} = 0.516 \, \omega_o a^2 \left(\frac{k_B T}{M\omega_o^2 u_o^2} \right)^2 \qquad (9)$$

where M is the atomic (C-H) mass, u_0 is the equilibrium amplitude of the distortion and ω_0 is the attempt frequency. In the double-well Y^4 theory considered by WS, ω_0 is the harmonic vibration frequency for an atom near the minimum of either well. In $(CH)_x$, we may take $\omega_0^2 = K/M$ where $K = 10.5$ eV/$Å^2$ is the spring constant.[50] Wada and Schrieffer[49] consider the interaction between neutral, free domain-walls and phonons. At room temperature using $M = 13$ AMU, $a \approx 1.4$ Å and $u_0 \approx 0.04$ Å, we find $D_{WS} \approx 2 \times 10^{-2}$ cm^2/sec $(D_{WS}/a^2 \approx 10^{14})$ in agreement with the measured[43] diffusion constant of the neutral magnetic solitons in undoped trans-$(CH)_x$.

In the case of charged solitons one might argue that the hopping attempt frequency is reduced by the Coulomb binding of the wall to the acceptor ion and assume that

$$D_{(CH)_x} = D_{WS} e^{-\Delta E/k_B T} \tag{10}$$

so that for lightly doped $(CH)_x$

$$\mu_{(CH)_x} = \frac{e}{k_B T} D_{WS} e^{-\Delta E/kT}$$

$$= 0.516 \left(\frac{e}{k_B T}\right) \omega_0 a^2 \left(\frac{k_B T}{M \omega_0^2 u_0^2}\right)^2 e^{-\Delta E/k_B T} \tag{11}$$

For the charged soliton, with $\Delta E \approx 0.3$ eV, $D_{(CH)_x} \approx 2 \times 10^{-7}$ at room

temperature leading to a mobility of $\mu_{(CH)_x} \simeq 10^{-5}$ cm^2/V-sec. Although

of the correct magnitude, such a picture would imply hopping between

impurity sites whereas the data indicate that the number of available sites

is much larger;[38] i.e. comparable to the number of carbon atoms per unit

length on the chain. A detailed understanding of the diffusion (and mobility)

of charged solitons is clearly lacking. However, we would anticipate that

the activation energy for motion of a charged soliton (on an otherwise

perfect chain) would be much greater than that of a neutral soliton.[13]

Theoretical study of the charged soliton mobility is required for further

progress.

The hopping mobility discussed above is appropriate to steady

state (dark) transport in the dilute limit. However, the transport mobility

appropriate to photogenerated carriers may be considerably higher. Since

a soliton-like distortion would be expected to form around a photogenerated

carrier only after a considerable time delay, the band mobility might be

appropriate. Particularly in junctions where the carriers are rapidly

swept out by the junction electric field, a mobility greater than or equal

to that found in the metallic state would be expected.

V. Summary and Conclusion

The transport data presented in this paper indicate three important

concentration regimes:

1) $y < 0.001$; the dilute limit where carriers introduced by

doping act independently

2) $0.001 < y < 0.01$; the transitional region

3) $y > 0.01$, the metallic state.

From analysis of the data, we have been able to draw specific conclusions
relevant to these three regimes.

In the dilute limit, the transport is via carrier hopping; the
mobility is small ($\sim 5 \times 10^{-5}$ cm^2/V-s) and activated ($\Delta E = 0.3$ eV).
This localized state hopping transport is consistent with the proposed
soliton doping mechanism. Based on the soliton interpretation of the
steady state (dark) transport in the dilute limit, it was argued that the
mobility appropriate to photogenerated carriers may be considerably
higher; i.e. greater than or equal to that found in the metallic state.

The semiconductor-metal transition is evident in $[CH(AsF_6)_y]_x$
and results in a qualitative change in temperature dependence of the
conductivity and finite zero temperature values above $y_c \simeq 0.01 - 0.02$.
For iodine doping the situation is somewhat less clear.

The transport mobility in $[CH(AsF_6)_y]_x$ increases dramatically
on going through the transitional region. This large increase (five to six
orders of magnitude) represents perhaps the clearest indication of a major
change in electronic structure and/or transport mechanism at the SM
transition.

The high mobility in the metallic state (~ 60 cm^2/V-sec assuming
complete charge transfer with one carrier per dopant molecule) provides
strong evidence of the validity of a band theory approach with delocalized
states in this disordered metallic polymer. Even in this context the

mobility is surprisingly large; the inferred values are comparable to the mobilities found in the best metals (e.g. for copper $\mu \sim 50$ cm^2/V-sec at room temperature).

The metallic state is described as metallic strands separated by thin potential barriers (typically $W < 20$ Å and $V_o < 10^{-2}$ eV). Electron transfer through the barriers is via tunneling at low temperatures, with activation over the barriers at higher temperature. The main effect of orientation appears to be to alter the properties of the barriers. In particular, doping oriented cis-(CH)$_x$ starting material leads to significant improvement in conductivity due to smaller barrier widths and lower barrier heights. Analysis of the temperature dependence of the conductivity within this model leads to an estimate of the intrinsic conductivity in heavily doped metallic $[CH(AsF_5)_y]_x$, $\sigma \simeq 4 \times 10^4$ Ω^{-1}-cm^{-1} at room temperature.

These and related transport results must be viewed in the context of the broad based experimental study of the chemical and physical properties of this new class of conducting polymers. The transport data provide insight into many aspects of the problem. However, detailed understanding of the doping mechanism, charge transport, electronic structure, and the semiconductor to metal transition will require combined input including, in particular, structural, optical and magnetic information.

TABLE 1

Comparison of four-probe and Montgomery results for
$\sigma_{\parallel}$ and $\sigma_{\perp}$ on oriented samples at room temperature.

	$l/l_o = 3.1$	4-Probe $(\Omega^{-1}\text{-cm}^{-1})$	Montgomery $(\Omega^{-1}\text{-cm}^{-1})$
cis-$[CH(AsF_5)_{.14}]_x$	$\sigma_{\parallel}$	2450	2350
	$\sigma_{\perp}$	-	377
cis-$[CHI_{.25}]_x$	$\sigma_{\parallel}$	1500	1620
	$\sigma_{\perp}$	-	203
trans-$[CH(AsF_5)_{.10}]_x$	$\sigma_{\parallel}$	1800	2800
	$\sigma_{\perp}$	120	220

TABLE 2

Barrier parameters obtained from analysis of low temperature data obtained with metallic $[CH(AsF_5)_y]_x$

Sample	ℓ/ℓ_0		T_1	T_0	W (Å)	V_0 (eV)
trans-$[CH(AsF_5)_{.10}]_x$	1.0	$\sigma_\parallel$	48.1	41.3	17 Å	7.2×10^{-3} (eV)
		$\sigma_\perp$	47.8	39.0	18 Å	7.5×10^{-3}
trans-$[CH(AsF_5)_{.10}]_x$	2.8	$\sigma_\parallel$	35.0	37.3	16 Å	5.8×10^{-3}
		$\sigma_\perp$	54.7	54.0	15 Å	7.2×10^{-3}
cis-$[CH(AsF_5)_{.14}]_x$	3.1	$\sigma_\parallel$	21.4	48.9	9.2 Å	3.5×10^{-3}

References:

1. Shirakawa, H., Louis, E. J., MacDiarmid, A. G., Chiang, C. K., and Heeger, A. J., Chem. Commun. 578 (1978); Chiang, C. K., Druy, M. A., Gau, S. C., Heeger, A. J., Shirakawa, H., Louis, E. J., MacDiarmid, A. G. and Park, Y. W., J. Am. Chem. Soc. 100, 1013 (1978)

2. Chiang, C. K., Fincher, C. R., Jr., Park, Y. W., Heeger, A. J., Shirakawa, H., Louis, E. J., Gau, S. C. and MacDiarmid, A. G., Phys. Rev. Lett. 39, 1098 (1977)

3. Chiang, C. K., Gau, S. C., Fincher, C. R., Jr., Park, Y. W., MacDiarmid, A. G. and Heeger, A. J., Appl. Phys. Lett. 33, 181 (1978)

4. Ozaki, M., Peebles, D., Weinberger, B. R., Chiang, C. K., Gau, S. C., Heeger, A. J. and MacDiarmid, A. G., Appl. Phys. Lett. 35, 83 (1979)

5. Shirakawa, H., Ito, T., Ikeda, S., Polym. J. 4, 460 (1973)

6. Fincher, C. R., Jr., Peebles, D. L., Heeger, A. J., Druy, M. A., Matsumura, Y., MacDiarmid, A. G., Shirakawa, H. and Ikeda, S., Solid State Commun. 27, 489 (1978)

7. Park, Y. W., Druy, M. A., Chiang, C. K., Heeger, A. J., MacDiarmid, A. G., Shirakawa, H. and Ikeda, S., Polymer Lett. 17, 195 (1979)

8. Grant, P. M. and Batra, I. P., Solid State Commun. 29, 225 (1978)

9. Weinberger, B. R., Kaufer, J., Heeger, A. J., Pron, A. and MacDiarmid, A. G., Phys. Rev. B 20, 223 (1979)

10. Goldberg, I. B., Crowe, H. R., Newman, P. R., Heeger, A. J. and MacDiarmid, A. G., J. Chem. Phys. 70, 1132 (1979)

11. Weinberger, B. R., Kaufer, J., Heeger, A. J. and MacDiarmid, A. G., Phys. Rev. Lett. (Submitted)

12. Rice, M. J., Phys. Lett. 71A, 152 (1979)

13. Su, W. P., Schrieffer, J. R. and Heeger, A. J., Phys. Rev. Lett. 42, 1698 (1979)

14. Tani, T., Gill, W. D., Clarke, T. C., and Street, G. B., Preprint, IBM Symposium on Conducting Polymers, March 29, 30, 1979

15. Chien, S. N., Heeger, A. J., Kiss, Z., MacDiarmid, A. G., Gau, S. C. and Peebles, D. L., Appl. Phys. Lett. (to be published)

16. Shirakawa, H. and Ikeda, S., Polym. J. 2, 231 (1971)

17. T. Ito, H. Shirakawa and S. Ikeda, Kobunshi Ronbunsha 5, #6 (1976) p. 470 (English edition)

18. Ito, T., Shirakawa, H. and Ikeda, S., J. Polym. Sci. Polym. Chem. Ed. 12, 11 (1974)

19. Ito, T., Shirakawa, H. and Ikeda, S., J. Polym. Sci. Polym. Chem. Ed. 13, 1943 (1975)

20. Shirakawa, H., Ito, T. and Ikeda, S., Die Macromoleculare Chemie 179, 1565 (1978)

21. Druy, M. A., Tsang, Chi-Hwa, Brown, N., Heeger, A. J. and MacDiarmid, A. G., J. Polym. Sci. Polym. Phys. Ed. (in print)

22. Karasz, F. E., Chien, J. C. W., Galkiewicz, R., Wnek, G. E., Nature (in press)

23. Shirakawa, H. and Ikeda, S., ACS-CSJ Chemical Congress, Honolulu, Hawaii, April 1-6 (1979)

24. MacDiarmid, A. G., and Heeger, A. J., Preprint, IBM Symposium on Conducting Polymers, March 29, 30 (1979)

25. Hsu, S., Signorelli, A., Pez, G. and Baughman, R., J. Chem. Phys. 68, 5405 (1978); Baughman, R. H. and Hsu, S. L., Polym. Lett. 17, 185 (1979)

26. Mihály, L., Pekker, S. and Jánossy, A., J. of Synthetic Metals (in press)

27. Salaneck, W. R., Thomas, H. R., Bigelow, R. W., Duke, C. B., Plummer, E. W., Heeger, A. J. and MacDiarmid, A. G., J. Chem. Phys. (in press)

28. Salaneck, W. R., Thomas, H. R., Duke, C. B., Paton, A., Plummer, E. W., Heeger, A. J. and MacDiarmid, A. G., J. Chem. Phys. 71, 2044 (1979)

29. Fincher, C. R., Jr., Ozaki, M., Tanaka, M., Peebles, D. L., Lauchlan, L., Heeger, A. J. and MacDiarmid, A. G., Phys. Rev. B 20, 1589 (1979)

30. Park, Y. W., Denenstein, A., Chiang, C. K., Heeger, A. J. and MacDiarmid, A. G., Solid State Commun. <u>29</u>, 747 (1979)

31. Kwak, J. F., Clarke, T. C., Greene, R. L. and Street, G. B., Solid State Commun. <u>31</u>, 355 (1979)

32. Chiang, C. K., Park, Y. W., Heeger, A. J., Shirakawa, H., Louis, E. J. and MacDiarmid, A. G., J. Chem. Phys. <u>69</u>, 5098 (1978)

33. Heikes, R., <u>Buhl International Conference on Materials</u>, edited by E. R. Shatz (Gordon and Breach, New York, 1974)

34. Chaikin, P. M. and Beni, G., Phys. Rev. B <u>13</u>, 647 (1976)

35. Ozaki, M., Peebles, D. L., Weinberger, B. R., Heeger, A. J. and MacDiarmid, A. G. (to be published)

36. Mott, N. F., Philos. Mag. <u>19</u>, 835 (1969); Mott, N. F., in <u>Festkörperprobleme</u>, edited by J. H. Queissen (Pergamon, New York, 1969), Vol. 9, p. 22; Ambegaokar, V., Halperin, B. I. and Langer, J. S., Phys. Rev. B <u>4</u>, 2612 (1971)

37. Hsu, S. L., Signorelli, A. J., Pez, G. P. and Baughman, R. H., J. Chem. Phys. <u>69</u>, 106 (1978); Shirakawa, H., Sasaki, T. and Ikeda, S., Chem. Lett. (Japan) p. 1113 (1978); Harada, I., Tasumi, M., Shirakawa, H. and Ikeda, S., Chem. Lett. (Japan) 1411 (1978)

38. As discussed above, the value $\rho_o \simeq 10^{-4}$ (2×10^{18} carriers per cm^3) for "undoped" <u>trans</u>-$(CH)_x$ was determined from the magnitude of the thermopower and independently verified from C vs V measurements on p-n heterojunctions. In our earlier paper (ref. 30) we estimated

$10^{-4} < \rho_o < 10^{-3}$ based on uncertainties at that time on the boundaries of the dilute regime. However, the insensitivity of the activation energy (ΔE) to y (see Fig. 4) below y = 0.001 clearly identifies this as the dilute regime. For y > 0.001, ΔE begins to fall dramatically indicative of the importance of dopant-dopant interactions. This independently demonstrates that ρ_o is well below 10^{-3} and implies that the number N of available sites is comparable to the number of carbon atoms per unit length in the polymer chain.

39. Montgomery, H. C., J. Appl. Phys. **42**, 2971 (1971)

40. Thermoelectricity: An Introduction to the Principles, edited by D. K. C. MacDonald, (John Wiley and Sons, Inc., New York and London) p. 115

41. Mihály, G., Vancsó, G., Pekker, S. and Jánossy, A., J. of Synthetic Metals (in press)

42. Seeger, K., Gill, W. D., Clarke, T. C., Street, G. B., Solid State Commun. **28**, 873 (1978)

43. Nechtschein, M., Devreux, F., Greene, R. L., Clarke, T. C. and Street, G. B., Phys. Rev. Lett. (Submitted)

44. Mott, N. F. and Twose, W. D., Adv. Phys. **10**, 107 (1961); Borland, R. in Mathematical Physics in One Dimension, ed. by E. N. Lieb and D. C. Mattis (Acad. Press, N. Y., 1966) p. 319

45. Sheng, P., Sichel, E. K. and Gittleman, J. I., Phys. Rev. Lett. **40**, 1197 (1978); Sichel, E. K., Gittleman, J. I. and Sheng, P., Phys. Rev. B **18**, 5712 (1978); Sheng, P., Phys. Rev. B (Submitted)

46. Wnek, G. E., Chien, J. C. W., Karasz, F. E., Druy, M. A., Park, Y. W., MacDiarmid, A. G. and Heeger, A. J., J. Polymer Sci.; Polymer Letts. Ed. 17, 779 (1979)

47. Fincher, C. R., Jr., Ozaki, M., Heeger, A. J. and MacDiarmid, A. G., Phys. Rev. B 19, 4140 (1979)

48. Takayama, H., Lin-Liu, Y. R. and Maki, K., Phys. Rev. B (Submitted)

49. Wada, Y. and Schrieffer, J. R., Phys. Rev. B 18, 3897 (1978)

50. Ooshika, Y., J. Phys. Soc. Japan 12, pp. 1238, 1246 (1957)

Figure Captions:

Figure 1: Thermopower (S) vs y for $[CH(I_3)_y]_x$ at room temperature.

Figure 2: Temperature dependence of the thermopower in heavily doped

metallic $[CH(AsF_5)_y]_x$

• • • $[CH(AsF_5)_{.147}]_x$: non-oriented

o o o $[CH(AsF_5)_{.095}]_x$: oriented, $l/l = 3.2$

Figure 3: Conductivity vs $\frac{1}{T}$ for $[CH(AsF_5)_y]_x$ for values of y spanning

the full doping regime.

Δ Δ Δ oriented sample $(l/l_0 = 3.1)$ $y = 0.14$

o o o non-oriented with y as indicated.

Figure 4: Activation energy vs y for $[CH(AsF_5)_y]_x$ and $[CH(I_3)_y]_x$.

o o o trans-$[CH(AsF_5)_y]_x$: data obtained from Fig. 3.

• • • trans-$[CH(I_3)_y]_x$: data obtained from ref. 35.

Figure 5: Room temperature conductivity vs y, in the dilute limit, for

$[CH(AsF_5)_y]_x$. The solid line has slope of unity indicating

that initially σ is approximately proportional to y.

Figure 6: Temperature dependence of the normalized conductivity of

heavily doped metallic $(CH)_x$

• • • $[CH(AsF_5)_{0.14}]_x$: $\sigma_{RT} = 2450 \ \Omega^{-1}$-$cm^{-1}$

o o o $[CH(I_3)_{.08}]_x$; $\sigma_{RT} = 1500 \ \Omega^{-1}$-$cm^{-1}$

Both samples were made from oriented cis starting material

with $l/l_0 = 3.1$.

Figure 7: Low temperature conductivity of the metallic samples of Figure 6.

Figure 8: Temperature dependence of normalized conductivity of metallic trans-$[CH(AsF_5)_{0.10}]_x$

$+$ $\sigma_{\parallel}$ with $\ell/\ell_o = 2.8$ $\sigma_{\parallel}(RT) = 1400 \ \Omega^{-1}\text{-cm}^{-1}$

$\times$ $\sigma_{\perp}$ with $\ell/\ell_o = 2.8$ $\sigma_{\perp}(RT) = 280 \ \Omega^{-1}\text{-cm}^{-1}$

$\bullet$ $\sigma_{\parallel}$ with $\ell/\ell_o = 1$ $\sigma_{\parallel}(RT) = 240 \ \Omega^{-1}\text{-cm}^{-1}$

$\circ$ $\sigma_{\perp}$ with $\ell/\ell_o = 1$ $\sigma_{\perp}(RT) = 230 \ \Omega^{-1}\text{-cm}^{-1}$

The data marked $\sigma_{\parallel}$ and $\sigma_{\perp}$ for $\ell/\ell_o = 1$ (unstretched) represent two independent samples cut at $90°$ from a non-oriented film.

Figure 9: Low temperature conductivity of the metallic sample of Figure 8.

Figure 10: Normalized temperature dependence of trans-$[CH(AsF_5)_y]_x$ for $\ell/\ell_o = 3.0$.

$\Delta \ \Delta \ \Delta$ $y = 0$

$\times \ \times \ \times$ $y = 0.004$

$\bullet \ \bullet \ \bullet$ $y = 0.008$

$\circ \ \circ \ \circ$ $y = 0.03$

$+ + +$ $y = 0.10$

Figure 11: Low temperature conductivity (normalized) vs concentration. The onset of finite conductivity vs $T \to 0$ is indicative of the semiconductor-metal transition

Figure 12: Transport mobility vs concentration (see text).

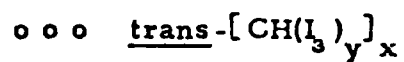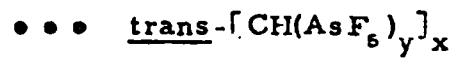● ● ● $\underline{trans}$-$[CH(AsF_6)_y]_x$

○ ○ ○ $\underline{trans}$-$[CH(I_3)_y]_x$

Figure 13: $-[\ln\sigma/\sigma_{RT}]^{-1}$ vs T; this plot allows evaluation of the
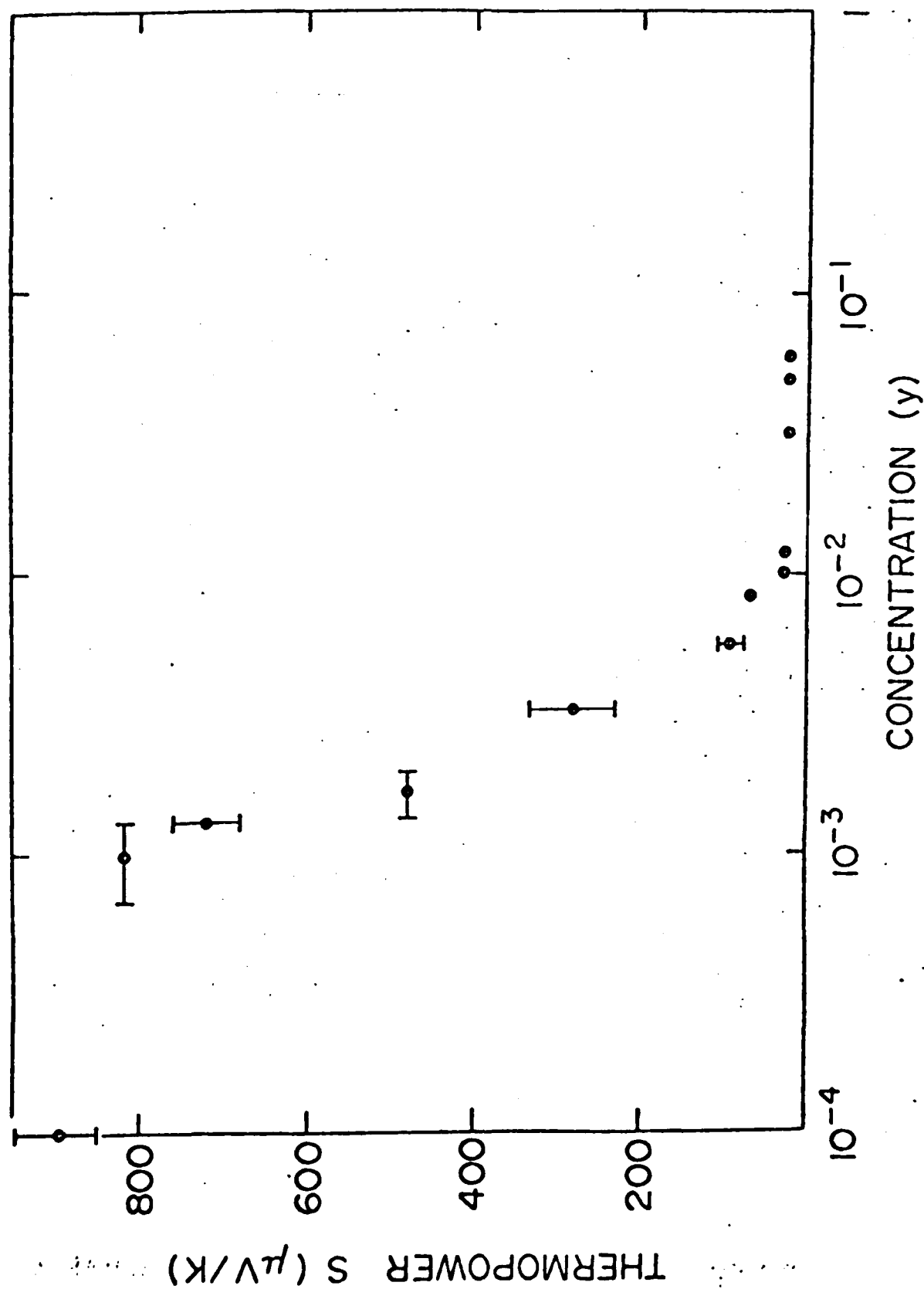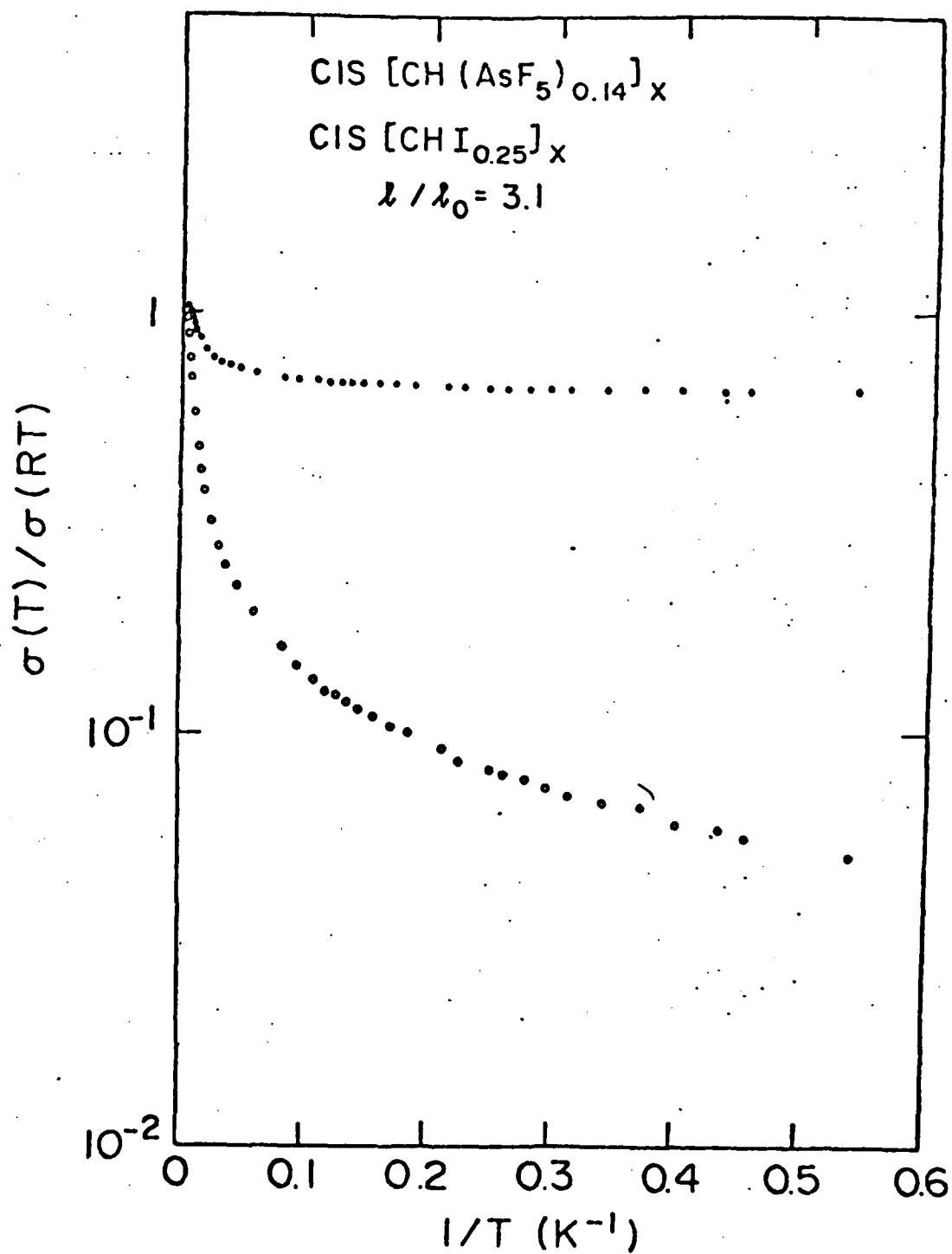
junction barrier parameters (see text).

Figure 1: Thermopower (S) vs y for $[CH(I_3)_y]_x$ at room temperature.

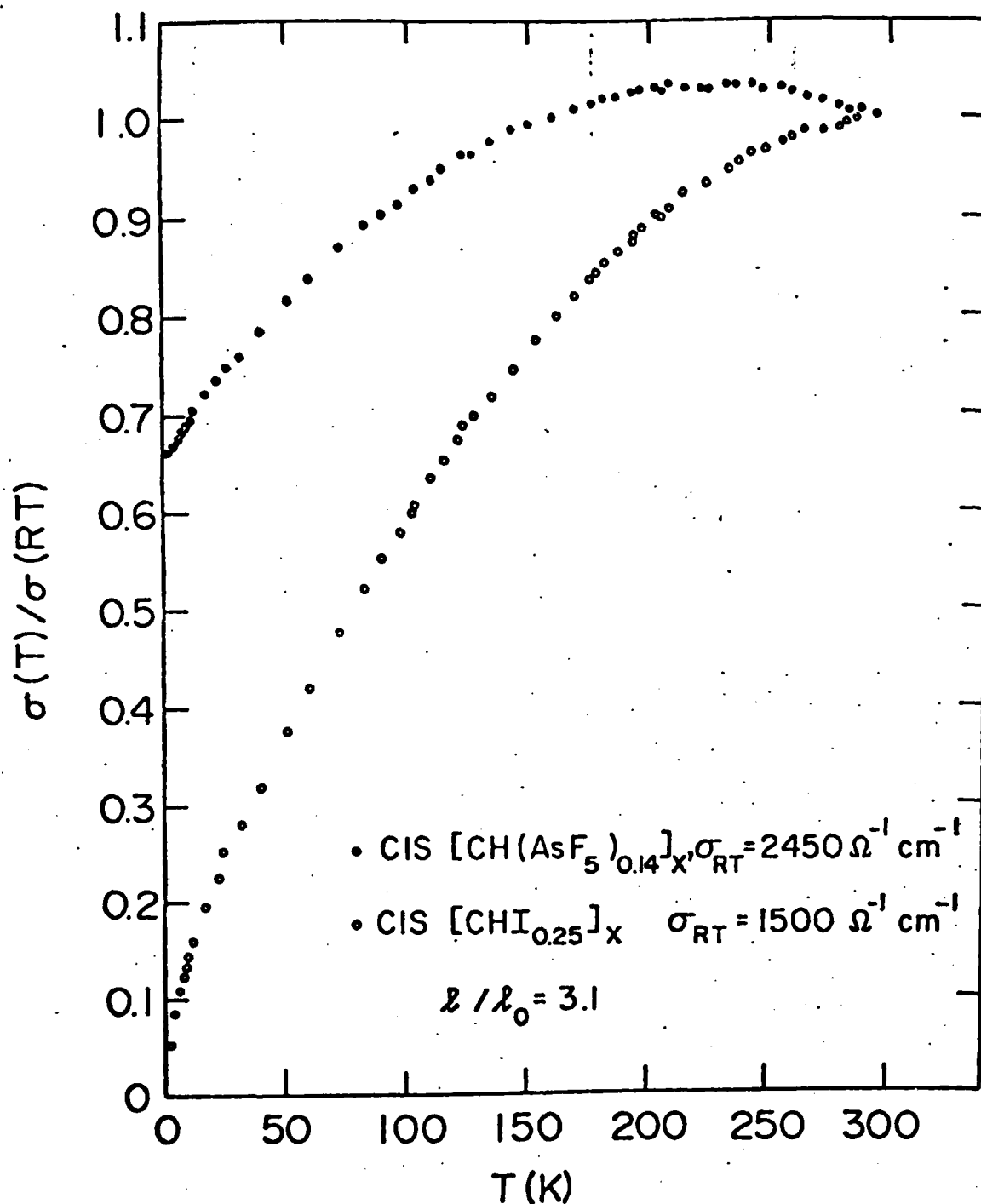Figure 7: Low temperature conductivity of the metallic samples of Figure 6.

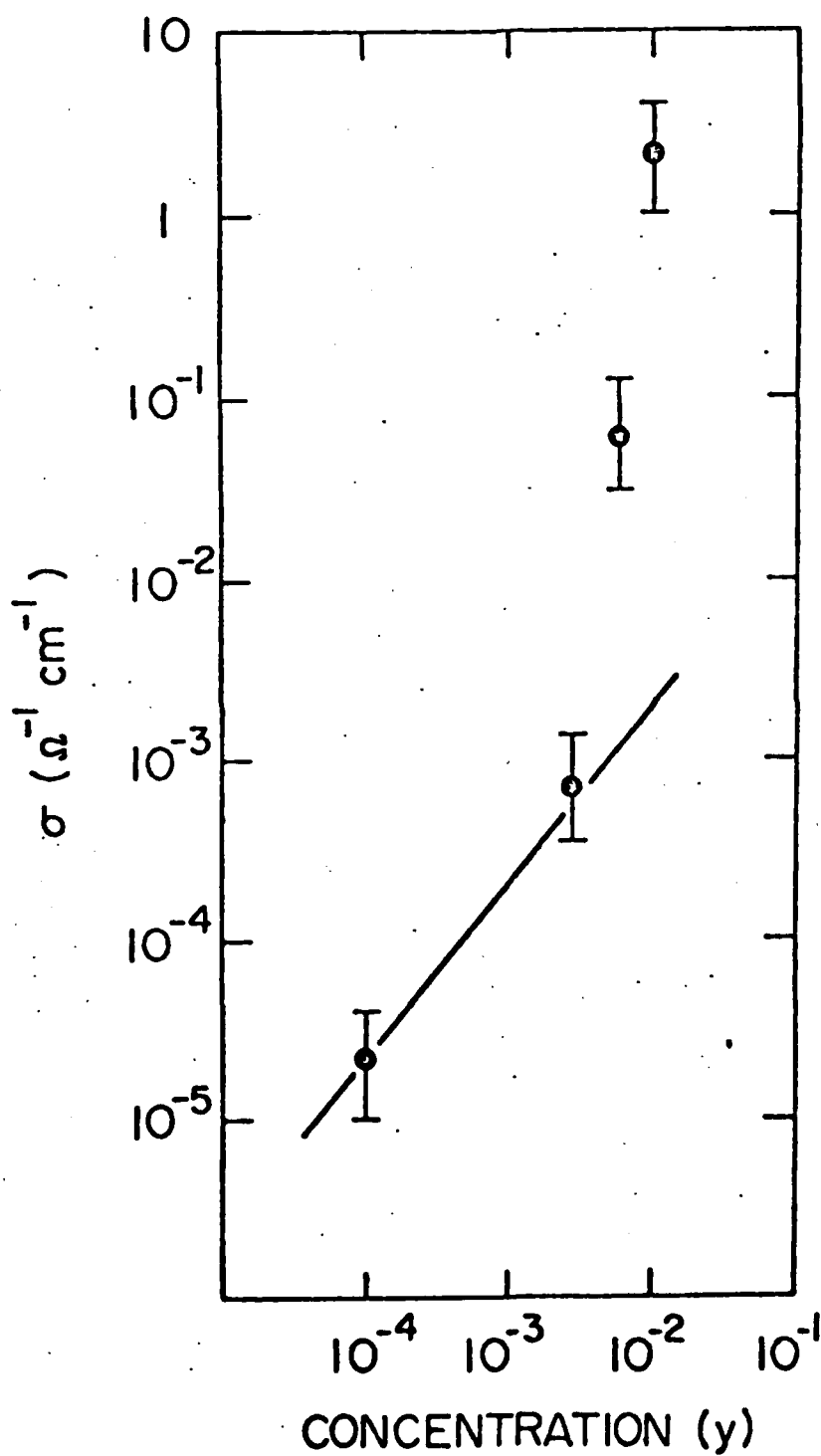**Figure 6:** Temperature dependence of the normalized conductivity of heavily doped metallic (CH)$_x$

$\bullet\bullet\bullet$ [CH(AsF$_5$)$_{0.14}$]$_x$; σ_{RT} = 2450 $\Omega^{-1}\cdot$cm^{-1}

$\circ\circ\circ$ [CH(I$_3$)$_{0.08}$]$_x$; σ_{RT} = 1500 $\Omega^{-1}\cdot$cm^{-1}

Both samples were made from oriented <u>cis</u> starting material with ℓ/ℓ_0 = 3.1.

Figure 5: Room temperature conductivity vs y, in the dilute limit, for $[CH(AsF_6)_y]_x$. The solid line has slope of unity indicating that initially σ is approximately proportional to y.

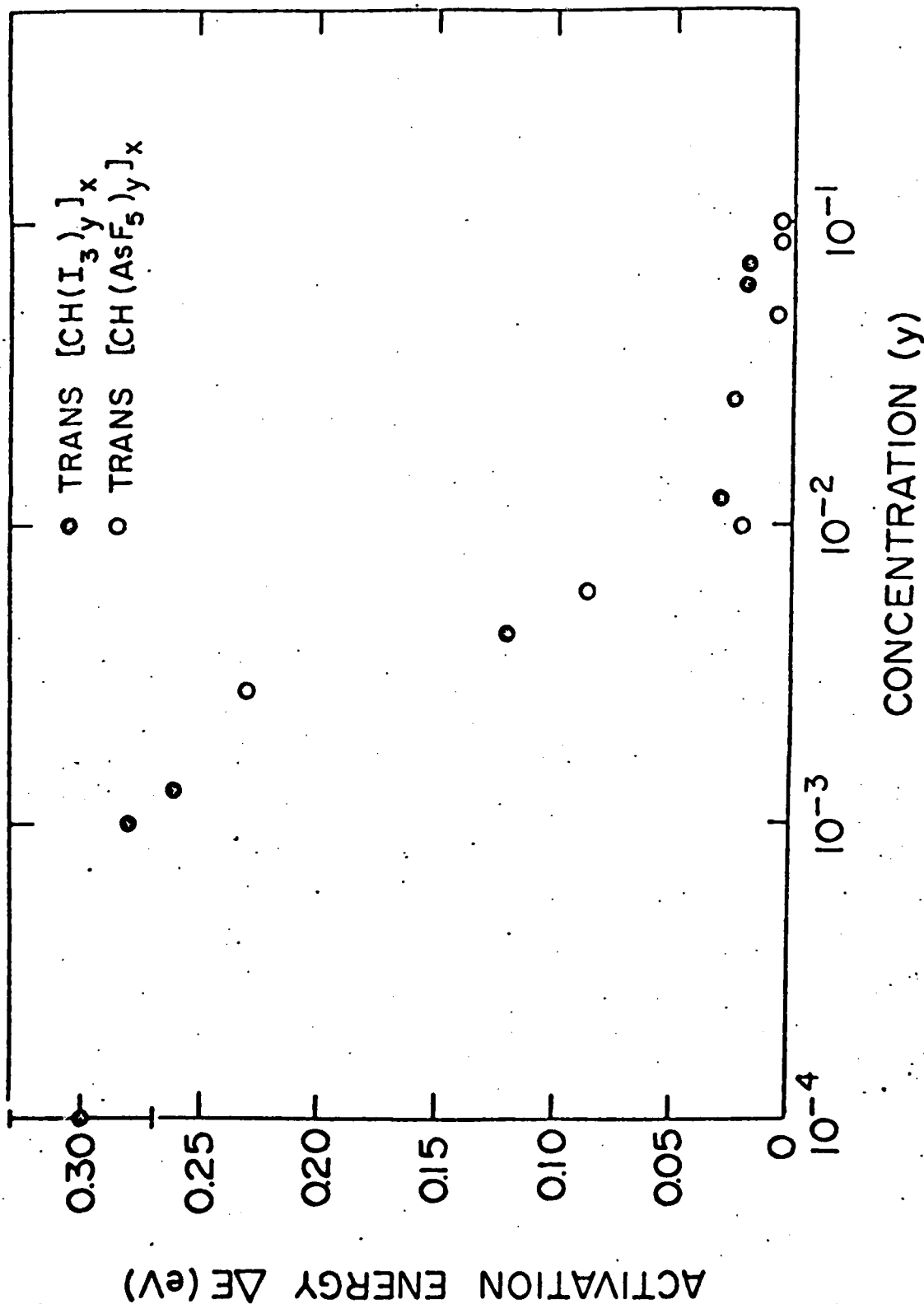Figure 4: Activation energy vs y for $[CH(AsF_6)_y]_x$ and $[CH(I_3)_y]_x$.

o o o <u>trans-$[CH(AsF_6)_y]_x$</u>; data obtained from Fig. 3.

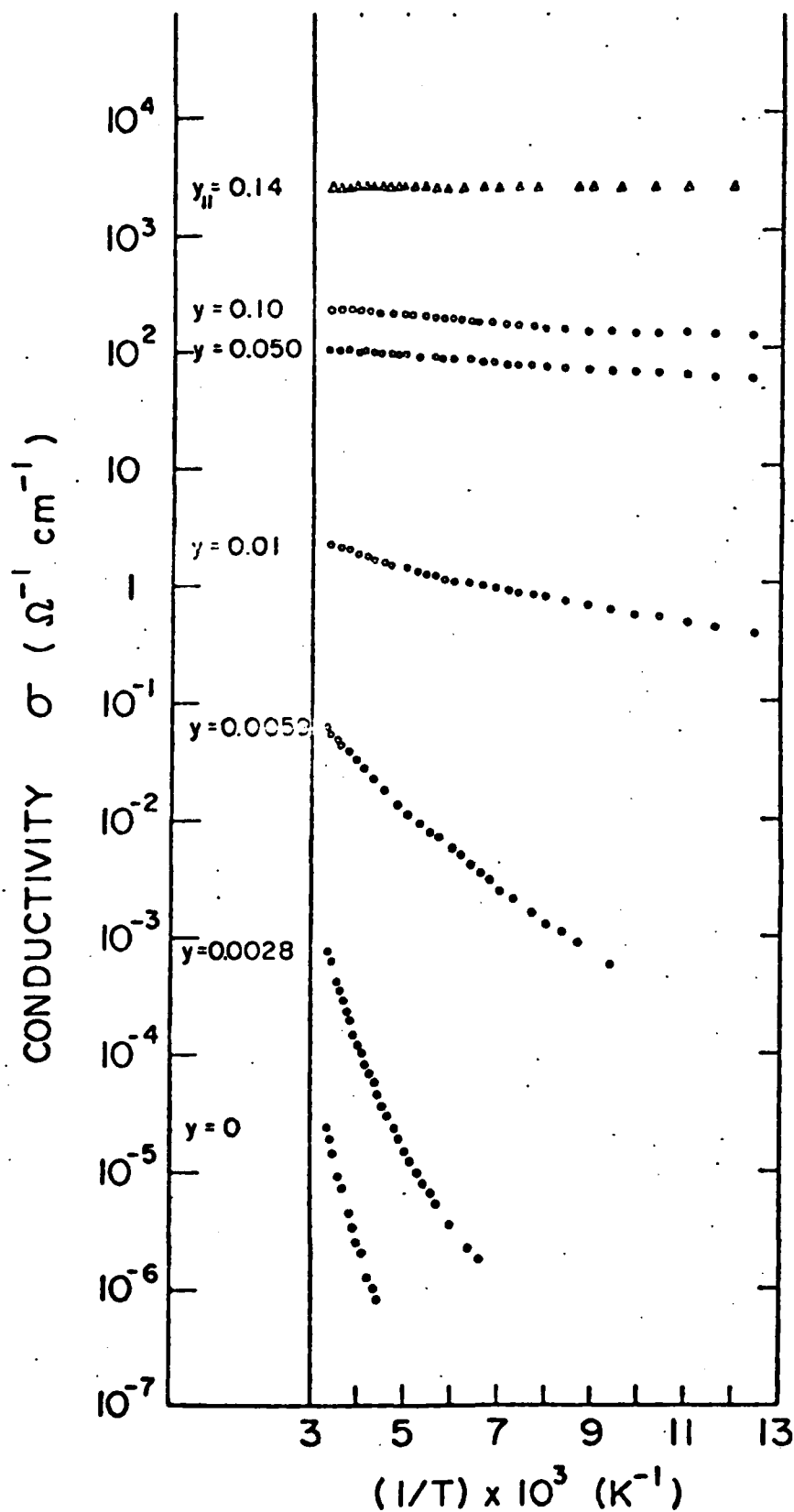• • • <u>trans-$[CH(I_3)_y]_x$</u>; data obtained from ref. 35.

Figure 3: Conductivity vs $\frac{1}{T}$ for $[CH(AsF_6)_y]_x$ for values of y spanning the full doping regime.

$\Delta\ \Delta\ \Delta$ oriented sample $(l/l_o = 3.1)$ y = 0.14

o o o non-oriented with y as indicated.

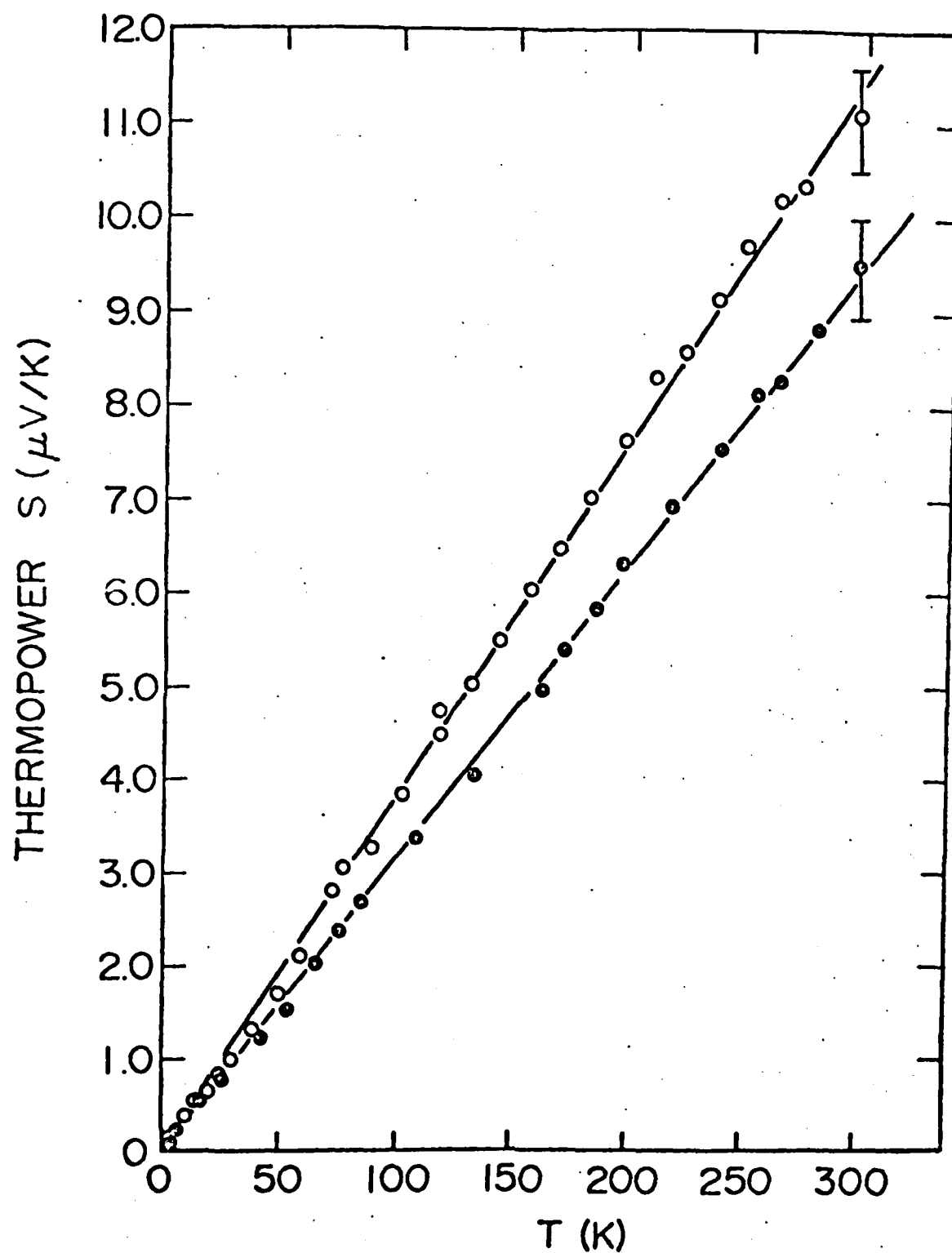Figure 2: Temperature dependence of the thermopower in heavily doped metallic $[CH(AsF_5)_y]_x$

● ● ● $[CH(AsF_5)_{.147}]_x$: non-oriented
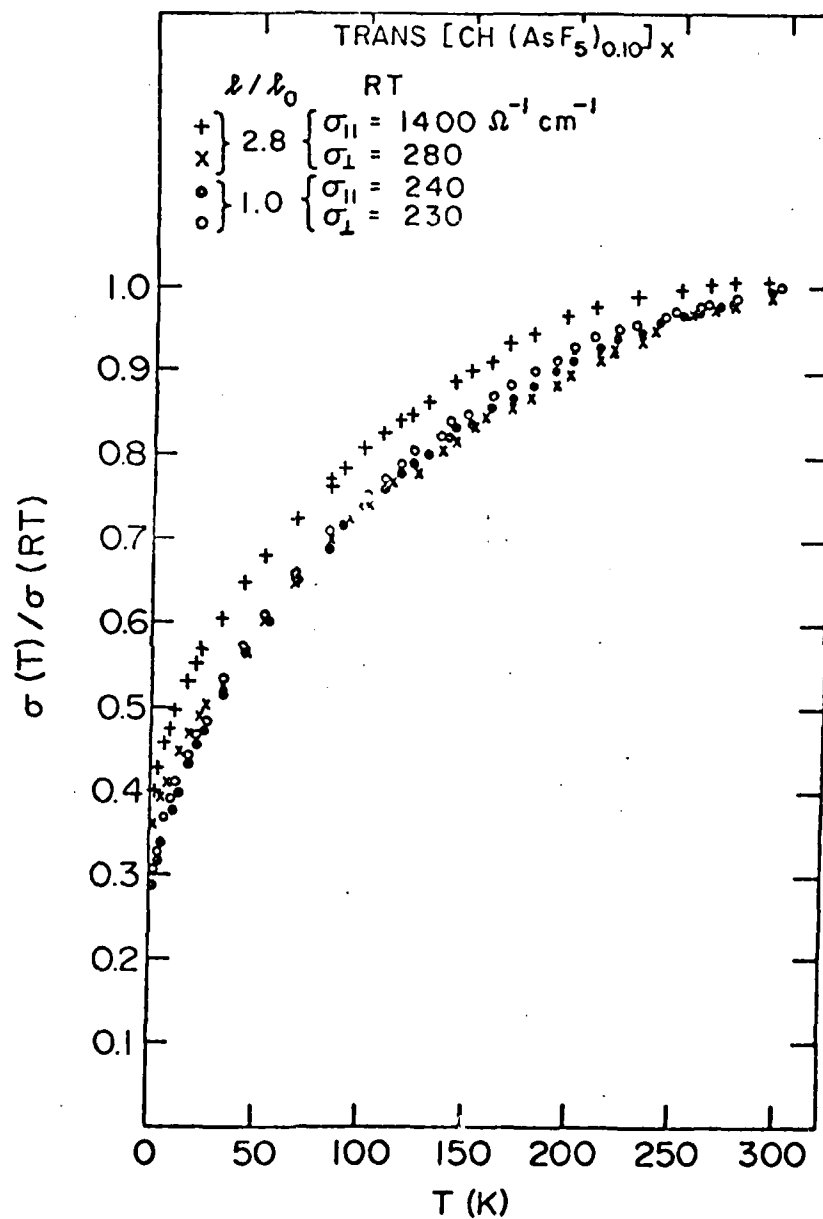
○ ○ ○ $[CH(AsF_5)_{.095}]_x$: oriented, $l/l = 3.2$

Figure 8: Temperature dependence of normalized conductivity of metallic
trans-$[CH(AsF_5)_{0.10}]_x$

+ $\sigma_\parallel$ with $l/l_0 = 2.8$ $\sigma_\parallel(RT) = 1400 \ \Omega^{-1}\text{-cm}^{-1}$

x $\sigma_\perp$ with $l/l_0 = 2.8$ $\sigma_\perp(RT) = 280 \ \Omega^{-1}\text{-cm}^{-1}$

• $\sigma_\parallel$ with $l/l_0 = 1$ $\sigma_\parallel(RT) = 240 \ \Omega^{-1}\text{-cm}^{-1}$

o $\sigma_\perp$ with $l/l_0 = 1$ $\sigma_\perp(RT) = 230 \ \Omega^{-1}\text{-cm}^{-1}$

The data marked $\sigma_\parallel$ and $\sigma_\perp$ for $l/l_0 = 1$ (unstretched) represent
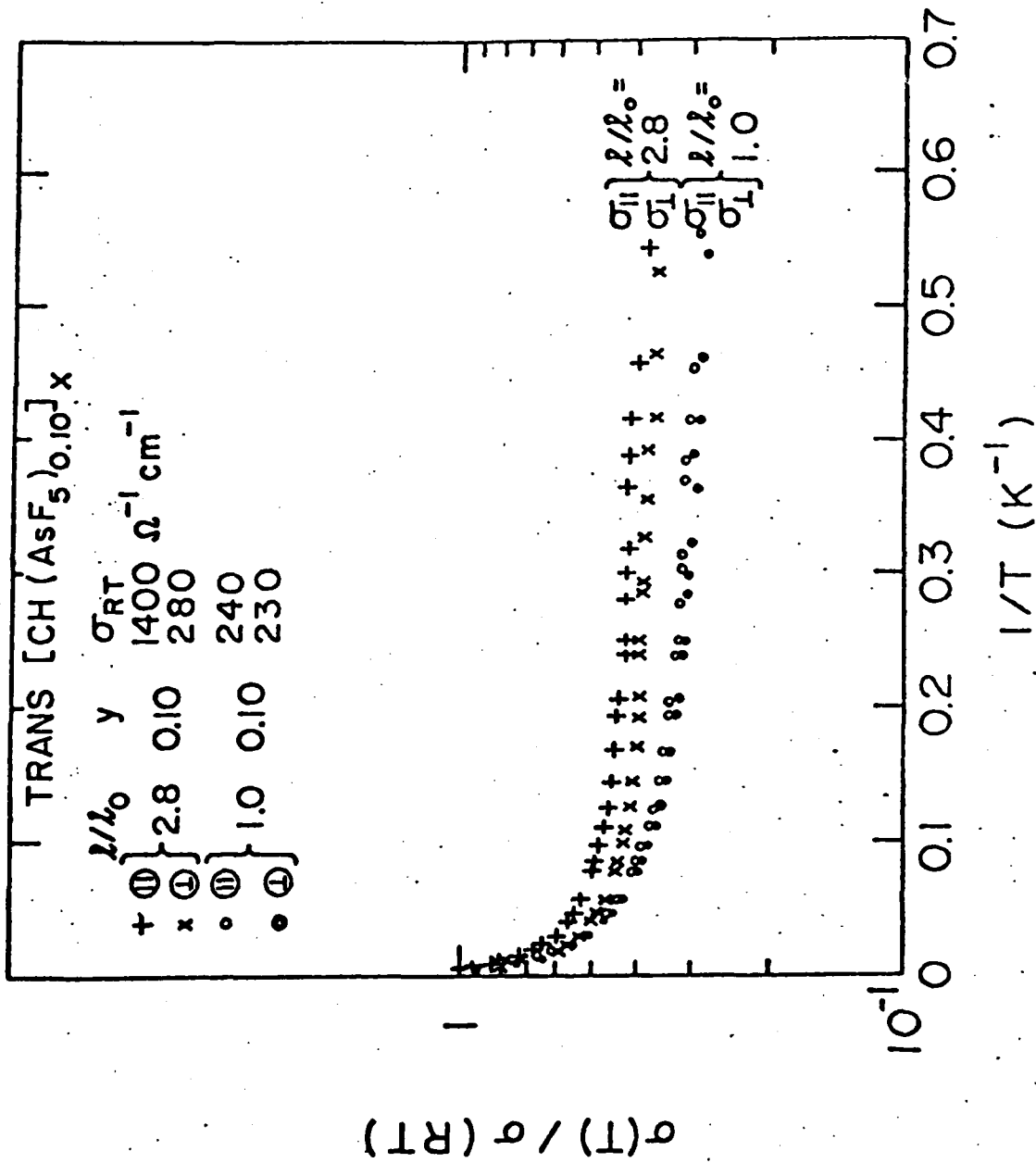two independent samples cut at $90°$ from a non-oriented film.

Figure 9: Low temperature conductivity of the metallic sample of

Figure 8.

Figure 10: Normalized temperature dependence of $\underline{trans}$-$[CH(AsF_5)_y]_x$ for $\ell/\ell_0 = 3.0$.

Δ Δ Δ			y = 0
x x x			y = 0.004
● ● ●			y = 0.008
o o o			y = 0.03
+ + +			y = 0.10

Figure 11: Low temperature conductivity (normalized) vs concentration.

The onset of finite conductivity vs $T \to 0$ is indicative of the

semiconductor-metal transition

Figure 12: Transport mobility vs concentration (see text).

• • •   trans-$[CH(AsF_5)_y]_x$

o o o   trans-$[CH(I_3)_y]_x$

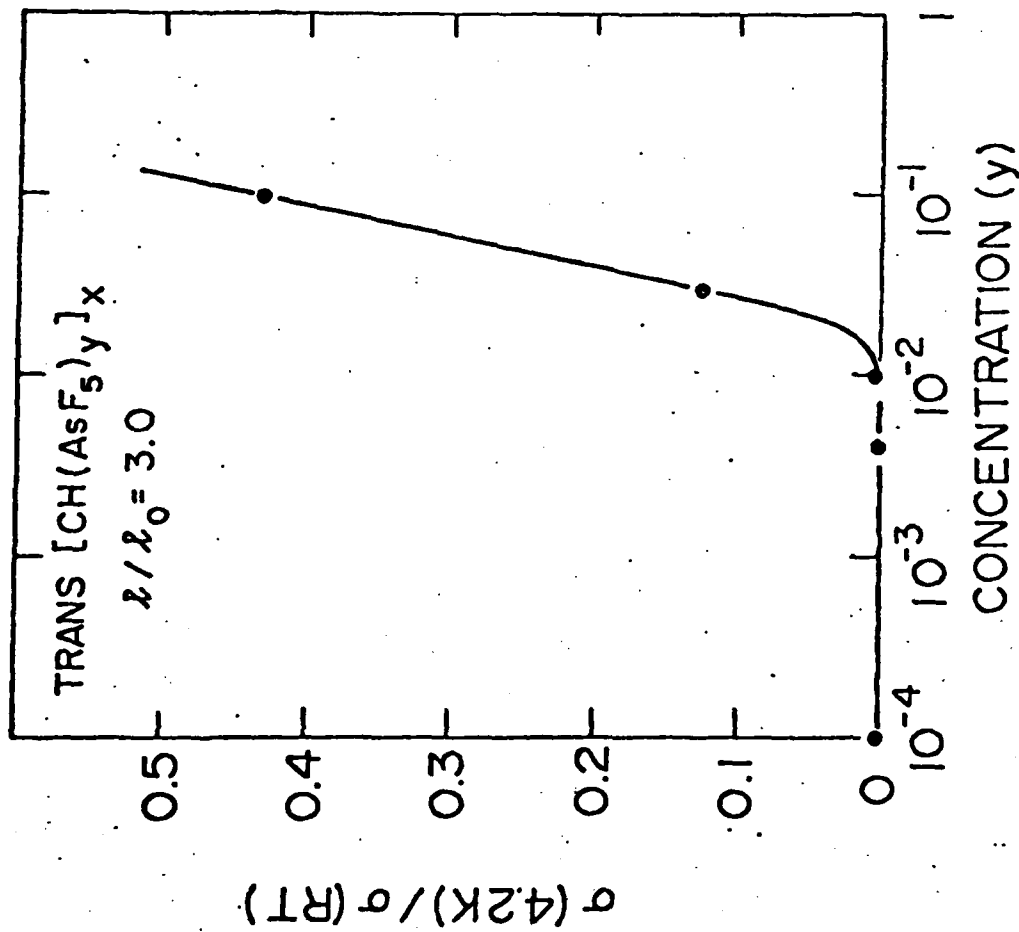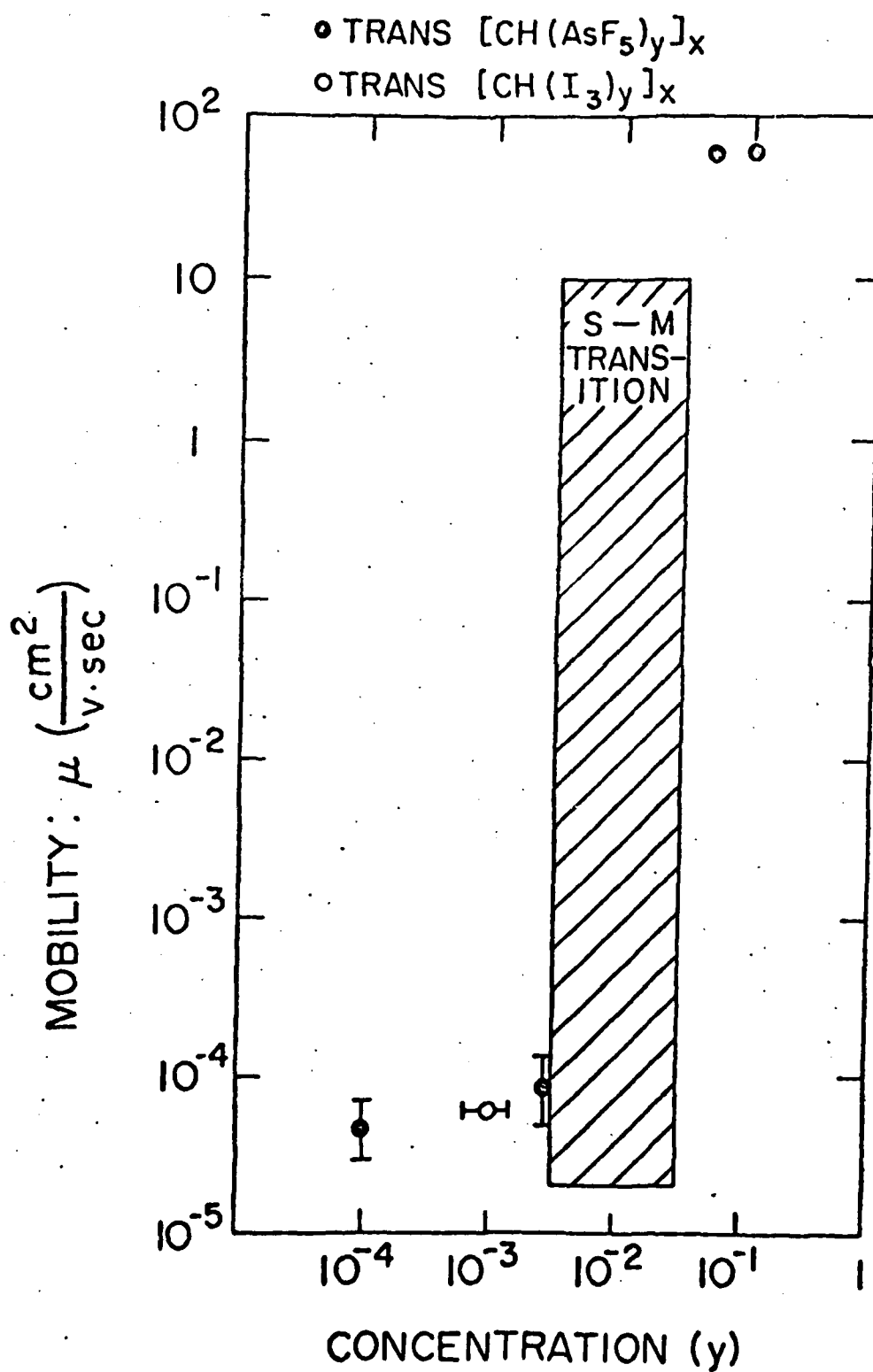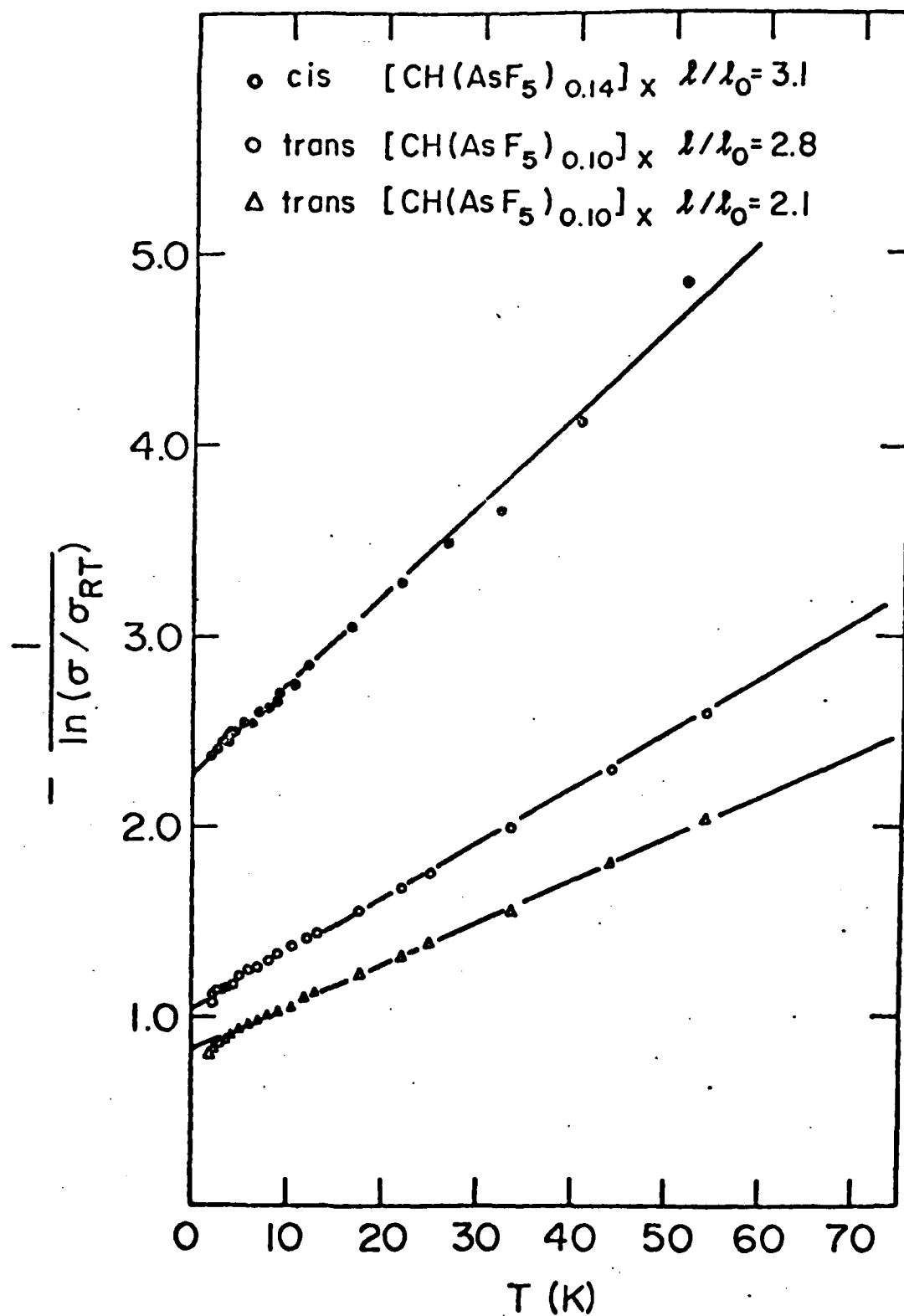Figure 13: $-[\ln\sigma/\sigma_{RT}]^{-1}$ vs T; this plot allows evaluation of the junction barrier parameters (see text).

TECHNICAL REPORT DISTRIBUTION LIST, GEN

	No. Copies		No. Copie

Office of Naval Research
Attn: Code 472
800 North Quincy Street
Arlington, Virginia 22217 — 2

ONR Branch Office
Attn: Dr. George Sandoz
536 S. Clark Street
Chicago, Illinois 60605 — 1

ONR Branch Office
Attn: Scientific Dept.
715 Broadway
New York, New York 10003 — 1

ONR Branch Office
1030 East Green Street
Pasadena, California 91106 — 1

ONR Branch Office
Attn: Dr. L. H. Peebles
Building 114, Section D
666 Summer Street
Boston, Massachusetts 02210 — 1

Director, Naval Research Laboratory
Attn: Code 6100
Washington, D.C. 20390 — 1

The Assistant Secretary
of the Navy (R,E&S)
Department of the Navy
Room 4E736, Pentagon
Washington, D.C. 20350 — 1

Commander, Naval Air Systems Command
Attn: Code 310C (H. Rosenwasser)
Department of the Navy
Washington, D.C. 20360 — 1

Defense Documentation Center
Building 5, Cameron Station
Alexandria, Virginia 22314 — 12

Dr. Fred Saalfeld
Chemistry Division
Naval Research Laboratory
Washington, D.C. 20375 — 1

U.S. Army Research Office
Attn: CRD-AA-IP
P.O. Box 1211
Research Triangle Park, N.C. 27709 — 1

Naval Ocean Systems Center
Attn: Mr. Joe McCartney
San Diego, California 92152 — 1

Naval Weapons Center
Attn: Dr. A. B. Amster,
Chemistry Division
China Lake, California 93555 — 1

Naval Civil Engineering Laboratory
Attn: Dr. R. W. Drisko
Port Hueneme, California 93401 — .

Department of Physics & Chemistry
Naval Postgraduate School
Monterey, California 93940 — 1

Dr. A. L. Slafkosky
Scientific Advisor
Commandant of the Marine Corps
(Code RD-1)
Washington, D.C. 20380 — 1

Office of Naval Research
Attn: Dr. Richard S. Miller
800 N. Quincy Street
Arlington, Virginia 22217 — 1

Naval Ship Research and Development
Center
Attn: Dr. G. Bosmajian, Applied
Chemistry Division
Annapolis, Maryland 21401 — 1

Naval Ocean Systems Center
Attn: Dr. S. Yamamoto, Marine
Sciences Division
San Diego, California 91232 — 1

Mr. John Boyle
Materials Branch
Naval Ship Engineering Center
Philadelphia, Pennsylvania 19112 — 1

TECHNICAL REPORT DISTRIBUTION LIST, 356B

<table>
<tr><td></td><td>No.
Copies</td><td></td><td>No.
Copies</td></tr>
<tr><td>Dr. T. C. Williams
Union Carbide Corporation
Chemical and Plastics
Tarrytown Technical Center
Tarrytown, New York</td><td>1</td><td>Douglas Aircraft Company
3855 Lakewood Boulevard
Long Beach, California 90846
Attn: Technical Library
C1 290/36-84
AUTO-Sutton</td><td>1</td></tr>
<tr><td>Dr. R. Soulen
Contract Research Department
Pennwalt Corporation
900 First Avenue
King of Prussia, Pennsylvania 19406</td><td>1</td><td>NASA-Lewis Research Center
21000 Brookpark Road
Cleveland, Ohio 44135
Attn: Dr. T. T. Serafini, MS 49-1</td><td>1</td></tr>
<tr><td>Dr. A. G. MacDiarmid
University of Pennsylvania
Department of Chemistry
Philadelphia, Pennsylvania 19174</td><td>1</td><td>Dr. J. Griffith
Naval Research Laboratory
Chemistry Section, Code 6120
Washington, D.C. 20375</td><td></td></tr>
<tr><td>Dr. C. Pittman
University of Alabama
Department of Chemistry
University, Alabama 35486</td><td>1</td><td>Dr. G. Goodman
Globe-Union Incorporated
5757 North Green Bay Avenue
Milwaukee, Wisconsin 53201</td><td>1</td></tr>
<tr><td>Dr. H. Allcock
Pennsylvania State University
Department of Chemistry
University Park, Pennsylvania 16802</td><td>1</td><td>Dr. E. Fischer, Code 2853
Naval Ship Research and
Development Center
Annapolis Division
Annapolis, Maryland 21402</td><td>1</td></tr>
<tr><td>Dr. M. Kenney
Case-Western University
Department of Chemistry
Cleveland, Ohio 44106</td><td>1</td><td>Dr. Martin H. Kaufman, Head
Materials Research Branch (Code 4542)
Naval Weapons Center
China Lake, California 93555</td><td>1</td></tr>
<tr><td>Dr. R. Lenz
University of Massachusetts
Department of Chemistry
Amherst, Massachusetts 01002</td><td>1</td><td>Dr. J. Magill
University of Pittsburg
Metallurgical and Materials
Engineering
Pittsburg, Pennsylvania 22230</td><td>1</td></tr>
<tr><td>Dr. M. David Curtis
University of Michigan
Department of Chemistry
Ann Arbor, Michigan 48105</td><td>1</td><td>Dr. C. Allen
University of Vermont
Department of Chemistry
Burlington, Vermont 05401</td><td>1</td></tr>
<tr><td>Dr. M. Good
Division of Engineering Research
Louisiana State University
Baton Rouge, Louisiana 70803</td><td>1</td><td>Dr. D. Bergbreiter
Texas A&M University
Department of Chemistry
College Station, Texas 77843</td><td>1</td></tr>
</table>

TECHNICAL REPORT DISTRIBUTION LIST, 356B

	No. Copies		No. Copies

Professor R. Drago
Department of Chemistry
University of Illinois
Urbana, Illinois 61801   1

Dr. F. Brinkman
Chemical Stability & Corrosion
  Division
Department of Commerce
National Bureau of Standards
Washington, D.C. 20234   1

Professor H. A. Titus
Department of Electrical Engineering
Naval Postgraduate School
Monterey, California 93940   1

COL B. E. Clark, Code 100M
Office of Naval Research
800 N. Quincy Street
Arlington, Virginia 22217   1

Professor T. Katz
Department of Chemistry
Columbia University
New York, New York 10027   1

Dr. Frank Karasz
Department of Polymer Science and
Engineering
University of Massachusetts
Amherst, Massachusetts 01003   1

Dr. James Chien
Department of Polymer Science and
Engineering
University of Massachusetts
Amherst, Massachusetts 01003   1

Professor A. J. Heeger
Director
Laboratory for Research on Structure
of Matter
33rd and Walnut Streets/K1
University of Pennsylvania
Philadelphia, Pennsylvania 19104   1

Dr. Richard A. Reynolds
Deputy Director
Defense Sciences Office
DARPA
1400 Wilson Blvd.
Arlington, Virginia 22209   1

Dr. Rudolph J. Marcus
Office of Naval Research
Scientific Liaison Group
American Embassy
APO San Francisco 96503   1

Mr. James Kelley
DTNSRDC Code 2803
Annapolis, Maryland 21402   1